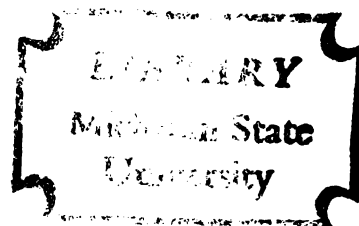DIFFUSION OF POLYELECTROLYTES IN
AQUEOUS SOLUTION

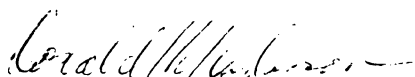Thesis for the Degree of Ph. D.
MICHIGAN STATE UNIVERSITY
Ernest E. Kern
1966

This is to certify that the

thesis entitled

"Diffusion of Polyelectrolytes in Aqueous Solution"

presented by

Ernest E. Kern

has been accepted towards fulfillment
of the requirements for

___Ph.D.___ degree in _Chemical_ Engineering

Major professor

Date_September 26, 1966

O-169

ABSTRACT

DIFFUSION OF POLYELECTROLYTES
IN AQUEOUS SOLUTION

by Ernest E. Kern

The diffusion of polyelectrolytes was studied in order to investigate the size and shape of the macromolecular ions in aqueous solution. The translational as well as the rotational diffusion coefficients were determined. The translational diffusion coefficients were measured by a very accurate optical method involving the use of an interferometer, and the rotational diffusion coefficients were determined by the measurement of the electrical anisotropy effect of the solutions in a shear field produced by a velocity gradient in the liquid.

Also of interest was the diffusional driving force as related to the electrostatic free energy of the counter ions and the polyions.

It was found that the diffusion coefficient for polyelectrolytes is much greater than the diffusion coefficient of nonionizing polymers, because of the greater mobility of the counterions as opposed to the mobility of the polyion.

In the diffusion of polymethacrylic acid it was observed that the polyion rapidly increased in size as the degree of neutralization was increased. The increase in the size of the polyion was attributed to the electrostatic repulsive forces between the charged groups on the polyion chain. It was also observed that at low concentrations the increase in size of the polyion occurred in two stages, whereas

at higher concentrations the opening of the polyion ocurred in one step. At the high concentrations the polyion does not open as far as it does at the low concentrations.

It was observed that the measured length of the polyion of polymethacrylic acid at a low concentration and high degree of neutralization approaches the fully extended length of the polyion indicating that polyion is nearly completely extended.

DIFFUSION OF POLYELECTROLYTES

IN AQUEOUS SOLUTION

By

Ernest E. Kern

A THESIS

Submitted to
Michigan State University
in partial fulfillment of the requirements
for the degree of

DOCTOR OF PHILOSOPHY

Department of Chemical Engineering

1966

To Christine

ACKNOWLEDGEMENT

TABLE OF CONTENTS

LIST OF FIGURES

LIST OF TABLES

INTRODUCTION

In a macroscopic state of equilibrium in the absence of external forces, the concentration of any molecular species, at constant temperature and pressure, is uniform throughout any single phase. If the distribution of molecules is not uniform, they will tend to move from regions of higher to those of lower concentration. Such a flow is a necessary condition of the second law of thermodynamics, since the entropy of the system is at a maximum when the molecules are distributed uniformly throughout. This process of flow, or diffusion results from the thermal energy of the molecules which gives rise to their Brownian movement. The speed with which the molecule diffuses is indicated by its diffusion constant which is in part a function of the size and shape of the molecule.

The Brownian movement of molecules involves both translation and rotation. The study of translational and rotational diffusion provides a good set of physical methods for investigating the size and shape of large molecules in solution.

In the determination of the translational diffusion constant, free diffusion is permitted to take place; while in rotational diffusion, the Brownian movement of the molecules is opposed by an external con- straining force, which tends to orient them. This orienting force may be a shearing force produced by a velocity gradient in the liquid. If the molecules are electric dipoles, the external force may be an electric field.

In order to better understand the rotational diffusion, let us
consider a system of ellipsoidal molecules in solution, whose
orientation may be described in terms of the angles between their
principal axes and some fixed direction in the surrounding medium.
If the molecules are oriented by an external force, so that their
principal axes are all parallel, and this orienting force is then
suddenly removed, the parallel orientation will gradually disappear.
In the final state of equilibrium, the distribution of orientations among
the molecules will be completely random. The rotational diffusion
constant is a measure of the speed with which this equilibrium is
approached.

In this study both the translational diffusion and rotational
diffusion constants of polyelectrolytes are investigated in order to
obtain the size and shape of the polyion of polymethacrylic acid. The
translational diffusion constants were measured with the use of a
Mach-Zehnder diffusiometer and the rotational diffusion coefficient
was determined by investigating the electrical anisotropy effect of the
polyelectrolyte solution.

Viscosity measurements were also made to verify the results
of the diffusion measurements.

THEORY

Diffusion

In 1855, Fick[11] suggested that the process of diffusion could
be treated as analogous to that of the conduction of heat. Fick's
law of diffusion also holds true for electrolyte solutions. This
law of diffusion is represented by the equation

$$J = - D(dc/dx)$$

for one-dimensional diffusion. J is the flux or rate of material
transfer across a plane of unit area and dc/dx is the concentration
gradient. D is the proportionality constant called the diffusion
coefficient.

The change of concentration with time at any point along the
diffusion cell in the x-direction is given by the relation

$$dc/dt = D \, d^2c/dx^2 \qquad (1)$$

which is Fick's second law.

These equations imply that D is independent of the
concentration. In general this is not true, but the analysis of
diffusion experiments is usually made on the assumption that D
can be treated as a constant over a narrow range of concentrations.

The diffusion of polyelectrolytes in an ionizing medium is unlike
the diffusion of other polymeric substances because of the presence
of ionized groups. The counterions of the polyelectrolyte have a much
greater mobility than the polyion. In order to maintain electrical
neutrality, the counterions exert a strong drag effect on the polyion,

3

thereby substantially increasing the diffusion rate above that of nonionizing polymers.

Nernst[36] showed that the differences in mobility of the positive and negative ions would tend to separate them during diffusion, which in turn would establish an electrostatic potential gradient within the diffusion cell. This gradient will have such a sign that it retards the faster ion and accelerates the diffusion of the slower.

Nagasawa and Fujita[37] have studied the concentration dependence of the diffusion coefficient of a polyelectrolyte in aqueous solution and have shown that the diffusion coefficient remains relatively constant except at very low concentrations. The diffusion coefficient of polystrenesulfonic acid was shown to drop off abruptly at infinite dilution.

Most diffusion studies of polyelectrolytes have been made with an added electrolyte. The added electrolyte eliminates the Nernst potential by suppressing the ionization of the counterions. Malmgren[35] determined the diffusion coefficient for polymeta-phosphates in 0.4 molar sodiumthiocyanate and obtained a value of 1.5×10^{-7} cm^2/sec. However Katchman and Smith[28] carried out the diffusion of polymetaphosphates in the absence of an added salt and observed the diffusion coefficient to be larger by a factor of 20 or more. Thus showing the effect of the counterions upon the Nernst potential and in turn the effect upon the diffusion coefficient.

One of the most interesting properties of polyelectrolyte solutions is the chain configuration as dependent on the degree of

ionization. The degree of ionization of a polyacid, such as poly-
methacrylic acid, can be controlled by the addition of a strong base.
The degree of ionization is related to the degree of neutralization
α, as shown by Wall.[19]

Katchalsky[24] observed that the viscosity of polymethacrylic
acid solutions increase 100 times as the degree of neutralization
increased from 0 to 50%. This increase in viscosity is caused by
the expansion of the polyion. The unionized macromolecules are
hypercoiled by intramolecular hydrogen bonding between the acid
groups and therefore are relatively small. Upon addition of sodium
hydroxide to the aqueous polyelectrolyte solution, the ionic dissociation
leads to large repulsive forces among the charged groups in the chain.
These repulsive forces give rise to an expanded configuration of the
polyion.

The diffusion of a solute in solution can be described by the
mutual diffusion coefficient, D, which is given by

$$D = \frac{1}{N\rho} \, n\left(\frac{d\mu}{dn}\right)_{P, T} \tag{2}$$

where n is the moles of solute per milliliter, ρ is the hydrodynamic
resistance of a single molecule, N is Avogadro's number, and μ is
the chemical potential of the solute. This equation also holds for
solutions of simple electrolytes. In this case:

$$\rho = \nu_1 \rho_1 + \nu_2 \rho_2$$

in which ν_1, ν_2 are the numbers of ions per molecule and ρ_1, ρ_2
are their hydrodynamic resistances.

The values of the hydrodynamic resistances are given by Stokes'[8] law

$$\rho = 6\pi\eta_o r \tag{3}$$

for a sphere of radius r, and

$$\rho = \frac{6\pi\eta_o a}{\ln 2a/b} \tag{4}$$

for a rod with length of $2a$ and thickness of b, where η_o is the viscosity of the medium.

From equations (2), (3) and (4) it can be seen that the diffusion coefficient for a polyelectrolyte varies inversely with the size of the polyion. Several investigators[24,26,38] have shown that the size of the polyion increases with increasing degree of ionization. The degree of ionization, a', for polymethacrylic acid is a function of the degree of neutralization, a. This relationship was studied by Huizenga, Grieger and Wall[19] who developed a diffusion method for determining the amount of counterion binding. They assumed that the mobility of the free ions (in their case sodium, Na^+) is the same as in simple electrolyte solutions and that the bound ions have no mobility, and then calculated the amount of ion binding, f, from the lowering of the apparent self-diffusion constant. Thus,

$$f = \frac{D_{Na}}{D_{Na}^*} \tag{5}$$

with D_{Na}, D_{Na}^* the self-diffusion constants of sodium ion in a simple salt solution and the polyelectrolyte solution, respectively.

The diffusion constant is easily measured by use of Na^{22}. In one compartment of a diffusion cell, which has a glass frit at the center, is placed a solution having no isotope, and in the other compartment is placed a solution having the same concentration but containing Na^{22}. The apparent diffusion constant can be calculated from the amount of Na^{22} transported across the glass frit in a given time by using Fick's law.

If f is the fraction of bound sodium ions then, $a' = a(1-f)$. The results are shown in Figure 1.

The term $n(d\mu/dn)$ in equation (2) is related to the osmotic pressure π by the Gibbs-Duhem equation:

$$n(d\mu/dn) = -n_s(d\mu_s/dn_s) \tag{6}$$

where the subscript s designates the sovlent. The osmotic pressure of the solution is:

$$\pi = -(1/v_s)(\mu_s - \mu_s^o) \tag{7}$$

where v_s is the molar volume of the solvent. From (6) and (7):

$$n(d\mu/dn) = n_s v_s(d\pi/n) \tag{8}$$

assuming a dilute solution, so that $n_s v_s = 1$ then,

$$n(du/dn) = (d\pi/dn) \tag{8a}$$

Katchalsky and Lifson[27] have shown that the osmotic pressure for a polyelectrolyte solution is given by the equation:

$$\pi = \phi(\nu + 1)nRT \tag{9}$$
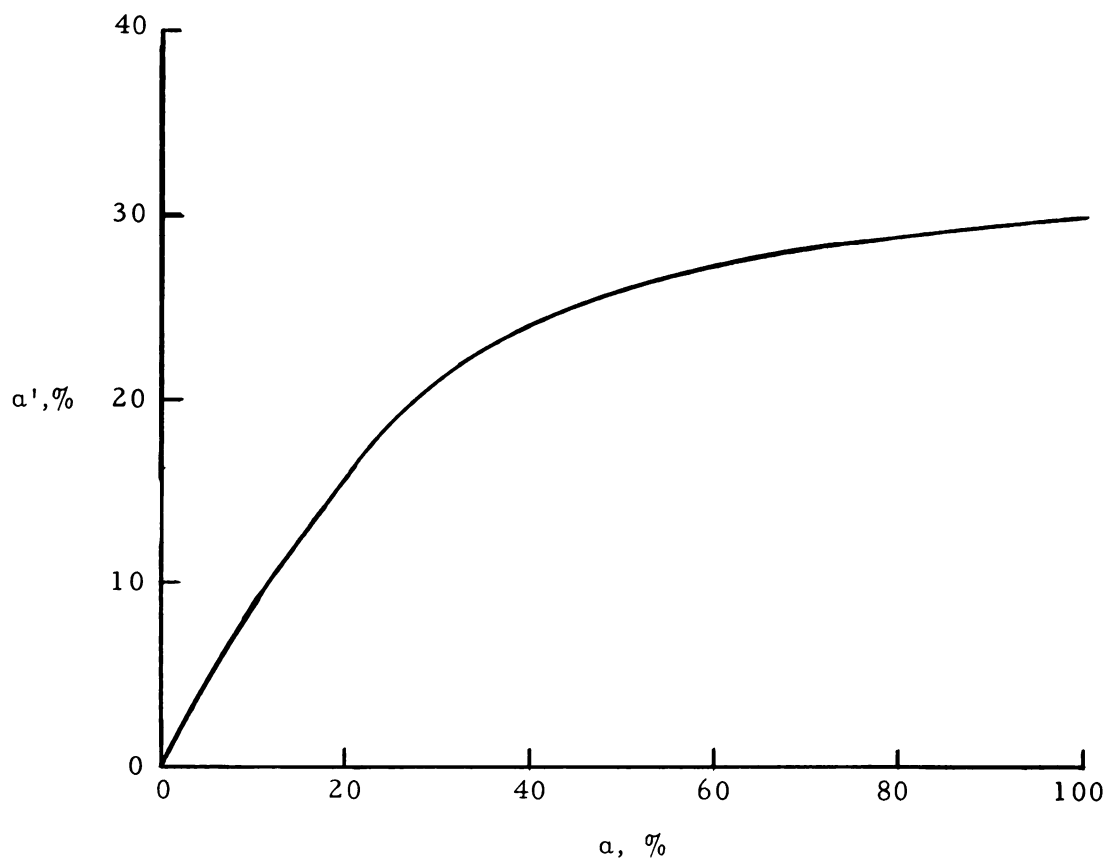
Figure 1. Degree of Ionization a' versus Degree of

Neutralization a .

where ϕ is the osmotic coefficient and ν is the number of ionized groups.

Differentiating (9) with respect to n and substituting into (2) one obtains the following:

$$D = \frac{kT}{\rho} \phi (\nu + 1) \left[1 + \frac{\partial \ln [\phi(\nu + 1)]}{\partial \ln \eta} \right] \qquad (10)$$

In the case where a substantial number of groups on the poly-ion are ionized $(\nu >> 1)$ and since the self-ionization of a weak acid is small within a wide range of concentration, so that $d\nu/dn = 0$, then equation (10) becomes:

$$D = \frac{kT}{\rho} \nu \left(\phi + \frac{\partial \phi}{\partial \ln \eta} \right) \qquad (11)$$

W. Kern[30] determined the osmotic coefficient of polyacrylic acid, in salt-free solution as a function of the degree of neutralization. His data are represented in Figure 2. This data in conjunction with (11) allow a qualitative determination of the diffusion coefficient.

A more theoretical approach would be to express the chemical potential of the solute in terms of electrostatic free energy of the solution. According to the interionic attraction theory it can be assumed that the chemical potential of an electrolyte in dilute solution may be separated into a term μ^{el} for the electrostatic interaction of the ions and a term $\mu^{o} + (\nu + 1)RT \ln m$ for the ideal behavior of a dilute solute which dissocated into $(\nu + 1)$ particles per molecule and where m is the molality.

The chemical potential of the solute and solvent are related to
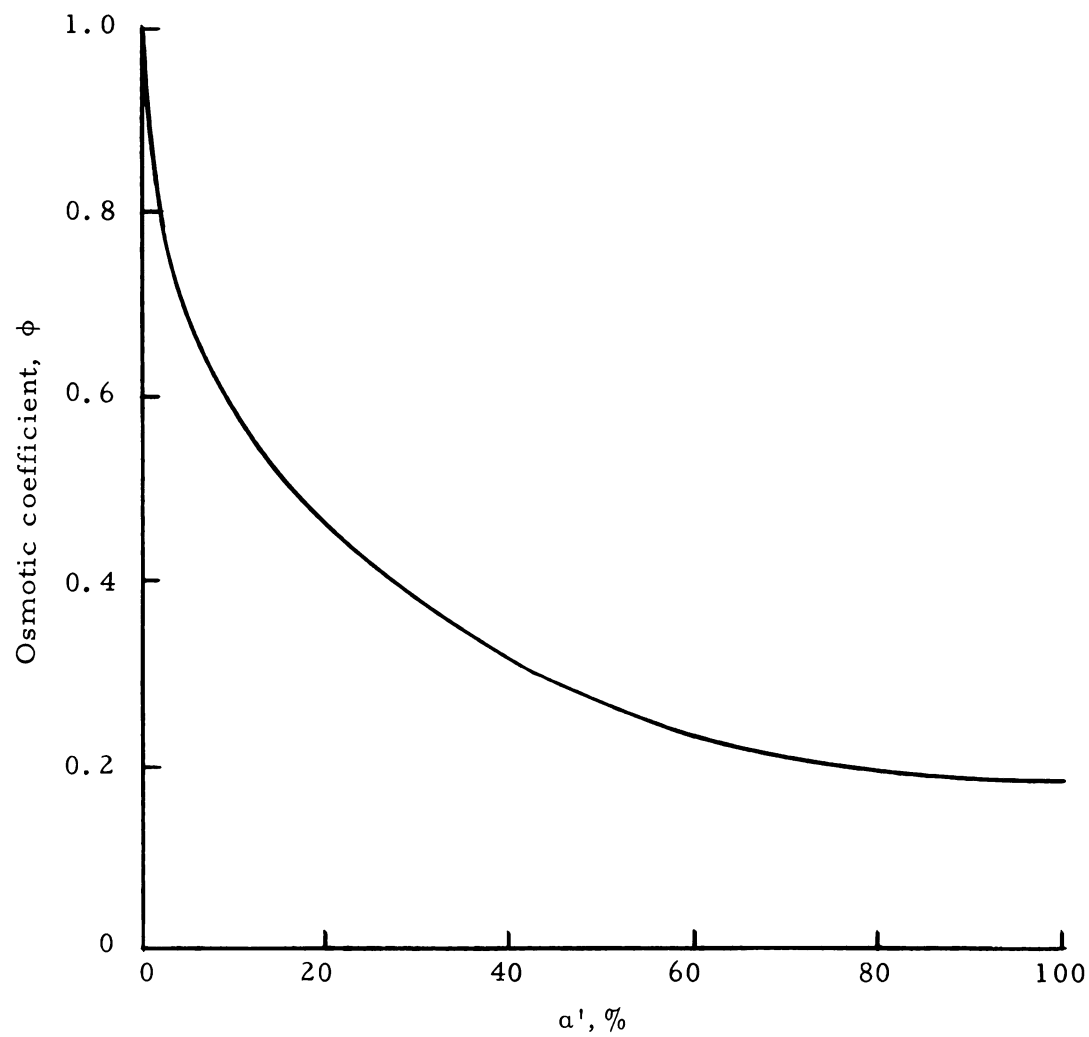
Figure 2.   Osmotic Coefficient of Counter Ions versus Degree
of Ionization.   From Reference (30).
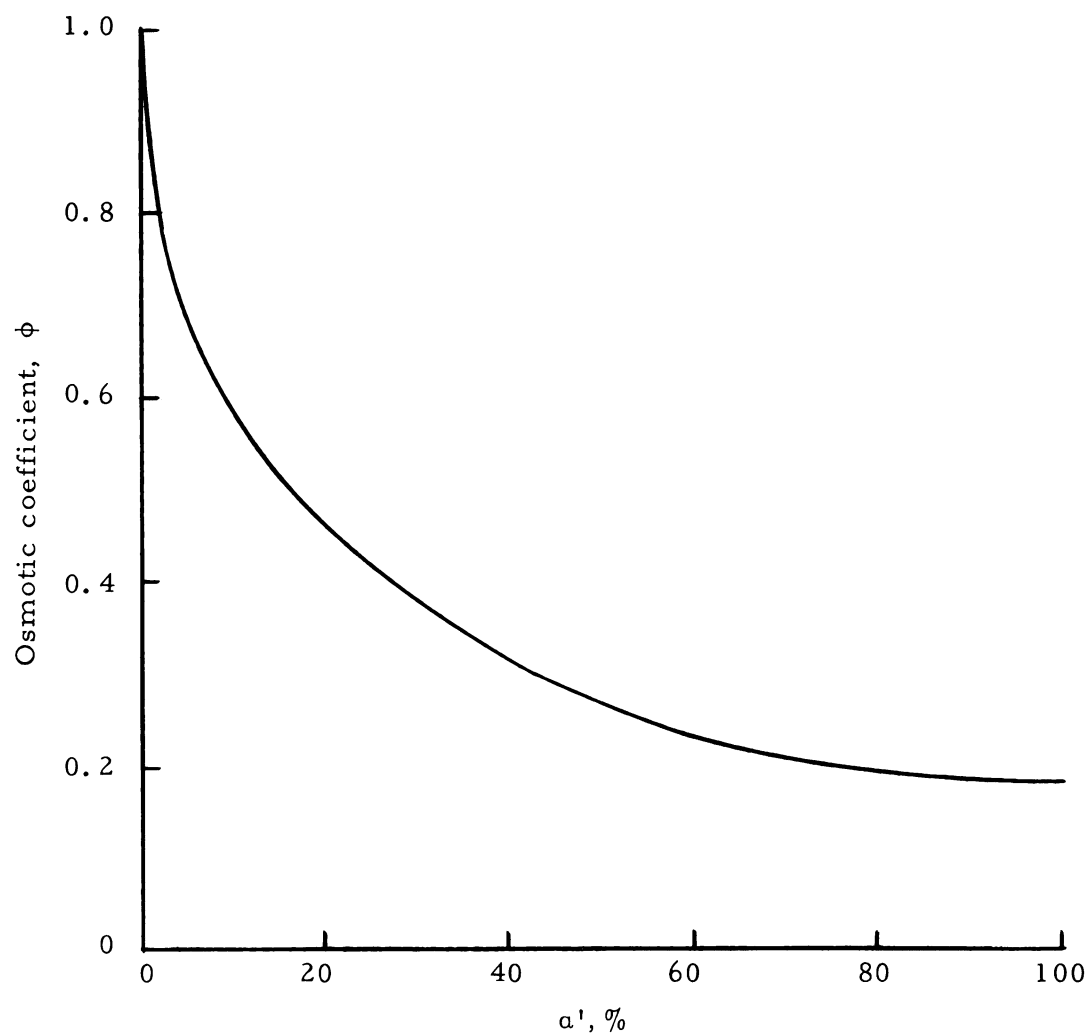
Figure 2.   Osmotic Coefficient of Counter Ions versus Degree of Ionization.   From Reference (30).

the total electrostatic free energy by the equation:

$$F_{el} = n_s \mu_s^{el} + n \mu^{el}$$

Neglecting the contribution of the solvent to the electrostatic free energy one obtains the following equation for the chemical potential of the solute.

$$\mu = \left(\frac{\partial F_{el}}{\partial n}\right)_{P, T} + \mu^{\circ} + (\nu + 1) RT \ln \frac{m}{1000} \qquad (12)$$

Katchalsky and Lifson[26] calculated the theoretical electrostatic free energy for a polyelectrolyte in dilute solution and further modifications were made by Harris and Rice.[16] The polyion was represented by a chain randomly coiled except for the electrostatic forces between its elements which were assumed to change only its mean square length. The reference state is assumed as the hypothetical state in which all ions carry no charge instead of the infinitely dilute state. This choice is made because the electrostatic interaction in the polyion does not vanish with dilution.

Debye's method of charging a system is used in the transition from the reference to the final state. This process is divided into three separate steps: (1) The macromolecules are stretched to their final end-to-end distance h and the free energy increased by F_1; (2) the ionic atmospheres are introduced at constant h increasing the free energy by F_2; (3) the fixed charges on the polyelectrolyte are allowed to interact which produces the repulsive free energy F_3.

According to Harris and Rice[16] the free energy of the first step will be:

$$F_1 = \frac{3}{2} kT \left(\frac{h^2}{h_o^2} - 1 \right) - 3 kT \ln \left(\frac{h}{h_o} \right) \qquad (13)$$

where h^2 is the average square end-to-end length of the polyion and h_o^2 is the unionized mean square length defined by Kuhn[32] as

$$h_o^2 = Z s b^2 \qquad (14)$$

where Z is the degree of polymerization, b the hydrodynamic length of a monomer, and s the numer of monomers per statistical element.

The free energy of the second step, which introduces the ionic atmospheres, is given by the Debye-Hückel expression:

$$F_2 = - \frac{\epsilon^2 \kappa \nu}{3 D_e} \qquad (15)$$

where ϵ is the electronic charge, ν is the number of fixed charged groups per macromolecule, D_e is the dielectric constant of the solvent, and κ is the reciprocal Debye radius which is given by

$$\kappa^2 = \frac{4 \pi \epsilon^2 \sum_i n_i}{D_e k T V_m} \qquad . \qquad (16)$$

where, V_m is the volume per macromolecule and n_i is the number of ions of type i per macromolecule.

The free energy attributed to the third step is due to the inter-action of the various charges on the polyion. If the interaction energy, u_{ij}, between a pair of charges on monomer units i and j a distance r_{ij} apart, is:

$$u_{ij} = \frac{\epsilon^2 \exp(-\kappa \gamma_{ij})}{D_e \gamma_{ij}} \tag{17}$$

Katchalsky[26] has shown that for a randomly coiled polymer of length h:

$$F_3 = \underset{i > j}{\Sigma} u_{ij} \cong \frac{\nu^2 \epsilon^2}{D_e h} \ln\left(1 + \frac{6h}{\kappa h_o^2}\right) \quad . \tag{18}$$

Later a better approximation was given by Rice:[16]

$$F_3 = \frac{\nu^2 \epsilon^2}{D_e} \left[\frac{6}{\kappa h_o^2} - \left(\frac{8}{3\pi}\right)^{1/2} \frac{h}{2} \left(\frac{6}{\kappa h_o^2}\right) + \ldots \right] \quad . \tag{19}$$

The over-all electrostatic free energy per macromolecule is given by the sum of the three steps.

$$F_{el} = F_1 + F_2 + F_3 = \frac{3}{2} kT \left(\frac{h^2}{h_o^2} - 1\right) - 3 kT \ln\left(\frac{h}{h_o}\right)$$
$$\tag{20}$$
$$- \frac{\epsilon^2 \kappa \nu}{3 D_e} + \frac{\nu^2 \epsilon^2}{D_e} \left[\frac{6}{\kappa h_o^2} - \left(\frac{8}{3\pi}\right)^{1/2} \frac{h}{2} \left(\frac{6}{\kappa h_o^2}\right)^2 + \ldots \right]$$

Since equation (20) represents the electrostatic free energy of the solute, then NF_{el} is the partial molar electrostatic free energy which is also equal to the electrostatic chemical potential of the solute. Therefore:

$$\mu_{el} = NF_{el} \quad .$$

Using the chain rule for derivatives and substituting equation (12) into

equation (2) we obtain

$$D = \frac{1}{\rho} \, \eta \left(N \, \frac{\partial F_{el}}{\partial h} \cdot \frac{\partial h}{\partial n} + \frac{(\nu + 1)RT}{\eta} \right) \tag{21}$$

where

$$\frac{dF}{dh} = \frac{3kT}{h_o^2} - \frac{3kT}{h} - \frac{\nu^2 \epsilon^2}{2D} \left(\frac{8}{3\pi}\right)^{1/2} \left(\frac{6}{h_o^2}\right) \quad . \tag{22}$$

With the information available it is not now possible to determine the

derivative dh/dn.

One can obtain the equilibrium end-to-end distance for the

macromolecule by minimizing the electrostatic free energy as given

in equation (20). Therefore setting

$$\left(\frac{dF_{el}}{dh} \right)_\nu = 0$$

we obtain:

$$\frac{3hkT}{h_o^2} - \frac{3kT}{h} = \frac{\nu^2 \epsilon^2}{2 D_e} \left(\frac{8}{3\pi}\right)^{1/2} \left(\frac{6}{\kappa h_o^2}\right)^2 \quad . \tag{23}$$

:

Electrical Anisotropy Effect

It is desirable to obtain the polyion dimensions by an independent means. The method of measuring the electrical anisotropy effect was chosen as described by Gotz[14] and Heckman.[17]

Anisometric particles which are electrically charged exhibit an anisotropic electrical conductivity if these particles are oriented by means of mechanical shear. The constant velocity gradient q, necessary to produce the shear field can be induced in the gap between the two concentric cyclinders of a Couette apparatus (Figure 14). The rotating cylinders produce an approximately uniform shear field between two sliding planes.

For anisometric particles, the probability of finding the longest principal axes of the ellipsoids in the direction of flow (Y) is a maximum, whereas for the shortest principal axes the probability is maximal in the direction of the velocity gradient (X). (Figure 3). Therefore as shown
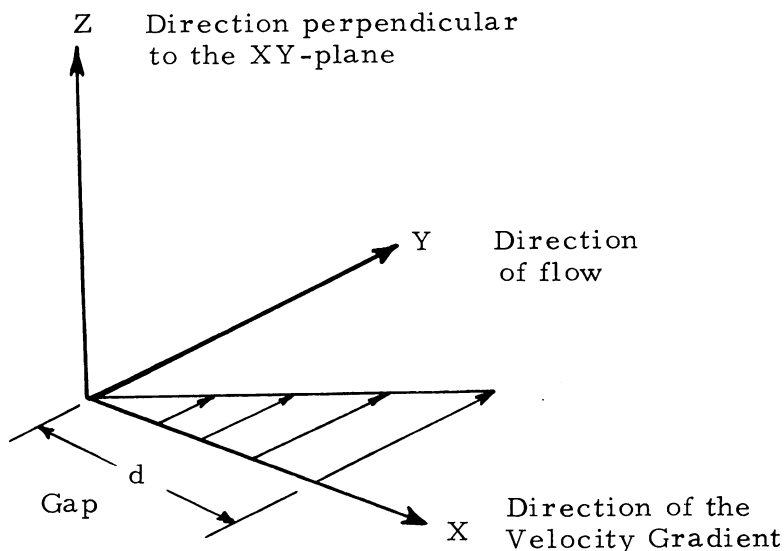
Figure 3. Vector Diagram in Gap of Couette Apparatus.

by Schwarz[42] the electrical conductivity of the solution will increase in the direction of flow.

For rod shaped particles the conductivity will decrease in the X and Z directions. In the case of complete orientation the conductivity change in the direction parallel to the axis of symmetry of the particle (i. e., in the direction of flow) is always twice the decrease in the perpendicular directions.

The smaller the particles, the greater the velocity gradient q must be in order to produce a partial orientation against the Brownian, rotational movement. In resting solutions the random movement is described by the rotational diffusion constant D_r

$$D_r = \frac{\bar{\phi}^2}{2t} \tag{24}$$

where $\bar{\phi}^2$ is the mean square value of a sufficiently small rotation ϕ that occurs in the time t around any axis perpendicular to the axis of symmetry.

The size of the particle can then be related to the rotational diffusion constant. Kuhn[31] and other investigators[13,40] derived an approximate relationship for rods and discs. For rods of length l:

$$l \text{ (cm)} = (8kT/\pi\eta_o D_r)^{1/3} \tag{25}$$

where k is the Boltzman constant, T the absolute temperature and η_o the viscosity of the solvent.

The rotational diffusion coefficient is determined by measuring the electrical conductivity of the polyelectrolyte solution in the direction of flow (Y) in the Couette apparatus as a function of the velocity gradient. (See pages 45 - 47.)

An anisometric particle in solution can be described approximately as a rotational ellipsoid with an axial ratio given by p. A rod corresponds to a stretched rotational ellipsoid with one long major axis and two short minor axes. Therefore p approaches infinity for a rod and b, the shape factor, approaches + 1, where

$$b = (p^2 - 1)/(p^2 + 1). \tag{26}$$

b is to be used later in determining the electrical anistropy.

The conductivity K_o of a solution at rest is proportional to the average particle mobility W_o.[9] W_o is composed of $W_\perp$ and $W_{||}$, which are the mobilities of the particle perpendicular and parallel to the major axis. Therefore

$$W_o = \frac{W_{||} + 2 W_\perp}{3} \tag{27}$$

If N is the number of polyions in a unit volume of solution and Q its effective charge, then according to equation (27) the greatest possible conductivity change is,

$$\bar{K} - K_o = \frac{2}{3} NQ^2 (W_{||} - W_\perp) . \tag{27a}$$

The qualitative dependence of the relative conductivity anisotropy upon σ , where σ is the ratio of velocity gradient to the rotational diffusion constant

$$\sigma = q/D_r \tag{28}$$

is given in Figure 4.
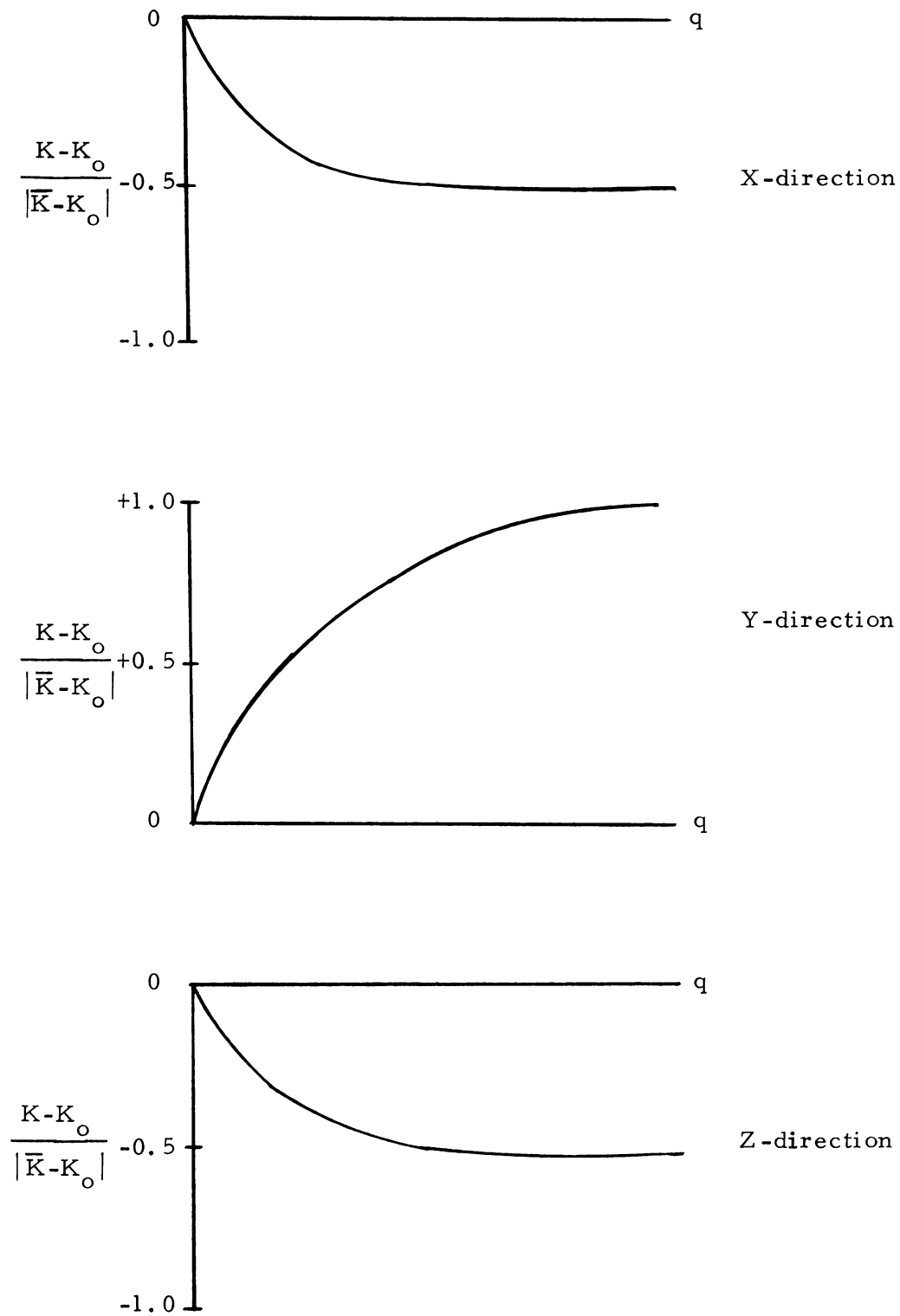
Figure 4.   Relative Anisotropy of Conductivity in X-, Y-, and

Z-directions as a Function of the Velocity Gradient

q, for Rod-Shaped Particles..

Heckman and Gotz[18] developed a relationship for the electrical conductivity anisotropy as a function of the rotational diffusion constant and the velocity gradient.

The velocity gradient developed in a gap of width d is given by

$$q(\sec^{-1}) = \frac{dV_y}{dx} = \frac{2\pi r(RPM)}{60d} \tag{29}$$

where r is the inner radius of the rotor. (Figure 14)

It is necessary to maintain laminar flow conditions but since the centrifugal force strongly stabilizes the laminar flow for the apparatus with the outer cylinder rotating,[43] the transition to turbulent flow occurs at relatively high Reynolds number. The critical gradient q_{max} up to which the flow remains laminar depends on the dimensions of the apparatus. Jerrard[23] showed that

$$q_{max}(\sec^{-1}) = f(r, d) \, \eta/\rho \tag{30}$$

where η/ρ is the kinematic viscosity of the solvent in stokes, and the function $f(r, d)$ is approximately 10^6 cm^{-2} for this system.

The particle is characterized by a shape factor b according to equation (26). The position of its major axis is described by the angles ϕ and γ (Figure 5) and its rotary movement by $\dot{\phi}$ and $\dot{\gamma}$. Therefore the axial flux, f, which flows in the volume angle $\Omega = \sin\gamma \, d\phi \, d\gamma$ is proportional to the angular velocity $\sin\gamma \cdot \dot{\phi}$ on the one hand and $\dot{\gamma}$ on the other hand. In the velocity gradient the particle performs an unsymmetrical rotational movement since $\dot{\phi}$ and $\dot{\gamma}$ are dependent upon the angle. Jeffery[22] derived this dependence for rotational ellipsoids:
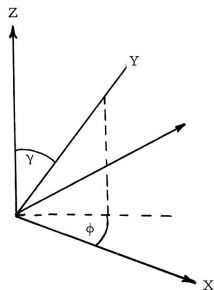
Figure 5.   Position of the Major Axis of the Particle, Coordinates γ and ϕ .
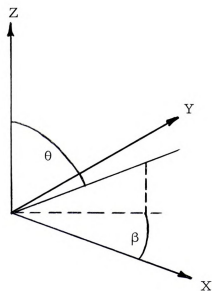
Figure 6.   Position of the Particle Relative to the Directional Measurement of Conductivity, Coordinates θ and β .

$$\dot{\phi} = \frac{1}{2} q (1 + b \cos 2\phi)$$

$$\dot{\gamma} = \frac{1}{4} q b \sin 2\gamma \sin 2\phi$$

(31)

Jeffery considers only the case where the Brownian movement is negligible and the orientation of the molecule is determined only by hydrodynamic forces.

According to Peterlin[39] one can now introduce a directional distribution function for the particle axes $\Phi(\phi, \gamma, t)$. If N is the number of particles per unit volume, dN the portion of particles found in the volume angle with orientation angles of ϕ, γ, then

$$\frac{dN}{N} = \Phi(\phi, \gamma, t) \, d\Omega$$

(32)

From the axial flux $f(\sin \gamma \cdot \dot{\phi}\dot{\gamma})$ and equation (32) there results the rotational flux of the particle, which results entirely from the flow:

$$\vec{J}_F = \Phi(\phi, \gamma, t) \cdot f(\sin \gamma \dot{\phi} \dot{\gamma})$$

(33)

The Brownian rotational movement opposes the orientation due to flow, the flux resulting from the Brownian movement is given by:

$$\vec{J}_D = - D_r N \text{ grad } \Phi(\phi, \gamma, t)$$

(34)

The time dependence of the particle density in the direction ϕ, γ is given by the continuity equation:

$$\frac{\partial \Phi}{\partial t} = - \text{div.} (\vec{J}_F + \vec{J}_D)$$

(35)

Since steady state is attained rapidly, $d\phi/dt = 0$, which gives the result that the two fluxes are equal but in opposite direction. There-

fore one obtains the solution to the directional distribution function as only dependent on $\sigma = q/D_r$ (equation (28)) and the shape factor b (equation (26)).

The relationship between the distribution function and conductivity anisotropy was recently examined by Schwarz.[42] For any directional measurement of conductivity the position of the particle is given by θ and β (Figure 6) and the relative change in conductivity is given by the equation:

$$\frac{K - K_o}{K_o} = \frac{1}{2} \left[(1 - 3 \cos^2 \theta) F_1 + \sin^2 \cos 2\beta \cdot F_2 + \sin^2 \theta \sin 2\beta \cdot F_3 \right] \left[\frac{\overline{K} - K_o}{K_o} \right] \quad (36)$$

where F_n (n = 1, 2, 3) are exponential series of the type:

$$F_n(\sigma) = k_n \sum_{i=1}^{\infty} l_{ni}(\sigma) b^i \qquad n = 1, 2, 3$$

the coefficient l_{ni} in the general case depends on t and the ratio $\sigma = q/D_r$, for the steady state case however, l_{ni} depends only on σ.

For $\sigma \leq \frac{1}{2}$, Schwarz[42] has shown that $F_3 = b\sigma/10$ and F_1, $F_2 = 0$. Therefore equation (36) reduces to

$$\frac{K - K_o}{K_o} = \sin^2 \theta \sin 2\beta \frac{b\sigma}{20} \cdot \frac{\overline{K} - K_o}{K_o} \quad (37)$$

Also for $\sigma \to \infty$ $F_1 = 1/2$, $F_2 = -3/2 b$ and $F_3 = 0$.

Heckman and Gotz[18] calculated the theoretical curves for the electrical anisotropy from equations (36), (37), and (38). By comparison of the experimental curve with the theoretical curve one can determine the rotational diffusion constant (see pages 45-47) and with equation (25) obtain the length of the particle.

EXPERIMENTAL METHOD

Diffusion Apparatus

The translational diffusion coefficients were determined with a Mach-Zehnder[34, 51] diffusiometer. The diffusiometer measures the refractive index of the solutions in a glass-windowed diffusion cell with an optical interferometer. The instrument was patterned after a similar diffusiometer described by Anderson,[1] Caldwell, Hall, and Babb[4, 5] and was constructed by Bidlack[2] for the study of the diffusion of binary nonelectrolyte liquid solutions. No modifications were necessary for the study of the diffusion of polyelectrolytes.

The Mach-Zehnder interferometer consists of a system of four mirrors positioned at the corners of a parallelogram. A schematic diagram in Figure 7 shows the location of the mirrors and other component parts. Mirrors 1 and 4 are half silvered mirrors which transmit one-half of the incident light beam and reflect the other one-half. Mirrors 2 and 3 are full reflectors.

The light beam originates from a Cenco quartz mercury arc lamp and is passed through a filter to isolate the 5461 $\overset{o}{A}$ green mercury line. The monochromatic light beam is then focused on a point source after which it passes through an achromatic lens to collimate the light beam. The collimated, monochromatic light is then split into two beams by mirror 1, half of the beam goes to the full-reflecting mirror 2 and the other half to the full-reflecting mirror 3. The two beams pass through the diffusion cell and are recombined at mirror 4. If the

24
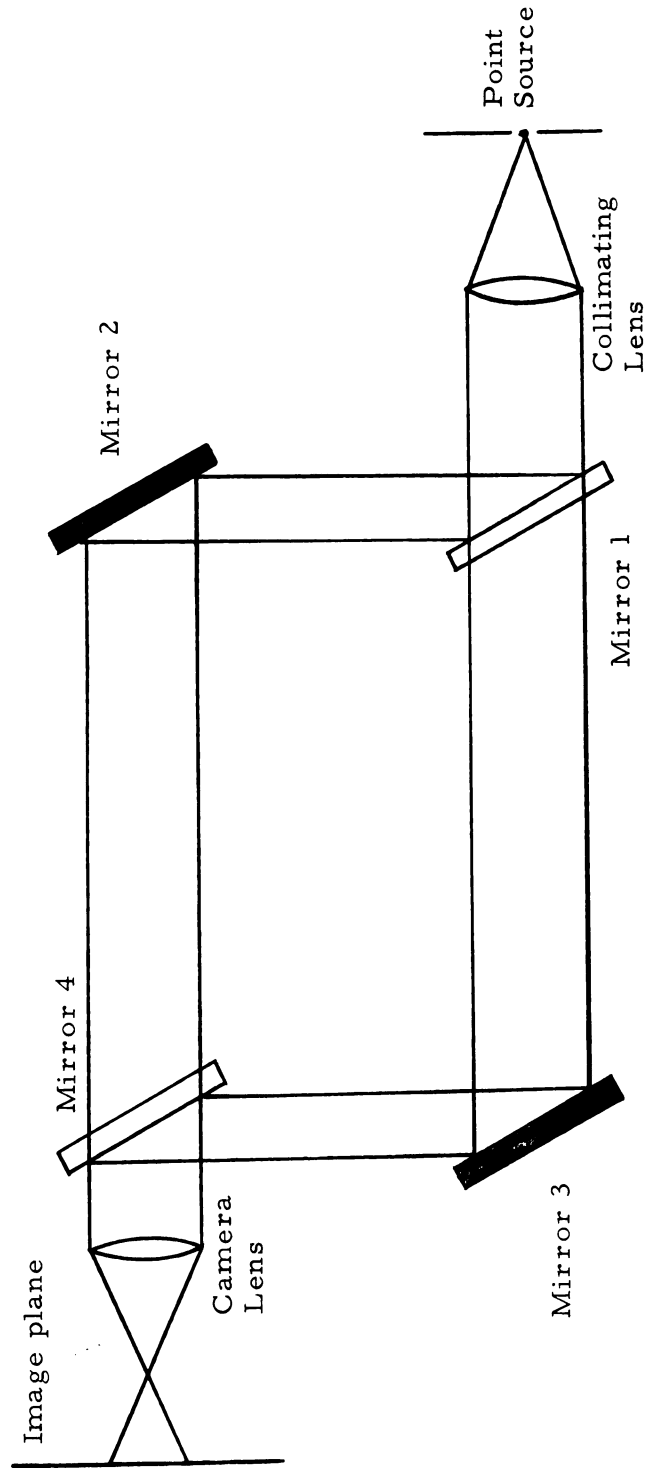
Figure 7. Schematic Diagram of Interferometer Showing Position of Mirrors.
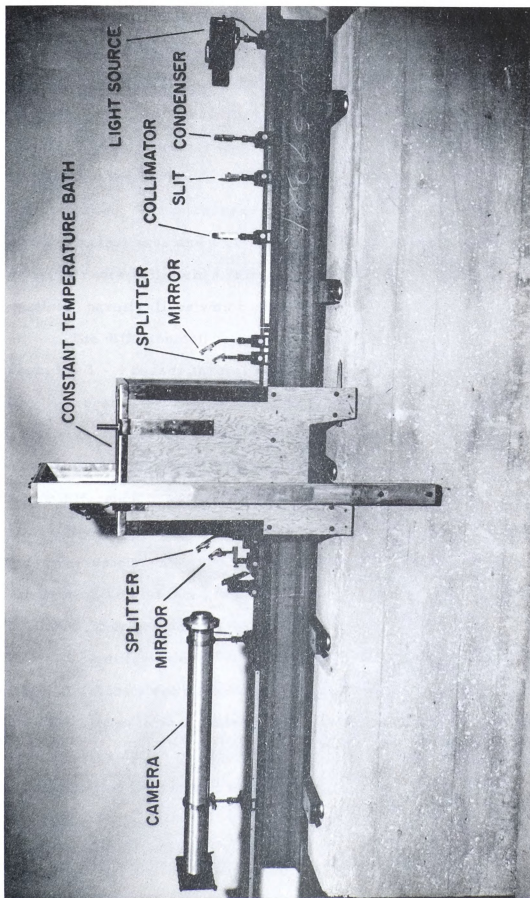
Figure 8. Photograph of Mach-Zehnder Interferometer Showing Components.

light path 1 - 2 - 4 is slightly different from the light path 1 - 3 - 4,
interference between the two beams will take place.

The interferences pattern is adjusted by a small rotation of
mirrors 1 or 2 about their axis in the plane of the paper to produce
straight line interference bands. If the path length difference
between the two beams is small the bands will be parallel and
evenly spaced. The mirrors are designed to also rotate about their
other principal axes and a combination of rotation and translation
of the mirrors will yield a fringe pattern which consists of straight,
vertical, parallel lines which are evenly spaced.

The diffusion cell is positioned in such a manner that light
beam 1 - 3 - 4 passes through the boundary between the two solutions.
The light beam 1 - 2 - 4 passes through a region in the cell where the
solution is of constant concentration and is therefore a reference beam.
The vertical fringes are displaced horizontally a distance proportional
to the difference in refractive index of the two solutions.[5] The resulting
fringe displacement pattern (Figure 9) is a direct plot of refractive
index versus distance. Thus if there is a vertical concentration
gradient in the cell this gradient may be followed by the amount of
horizontal displacement of the fringes.

The diffusion cell (Figures 10 and 11) consists of a channel cut
into a stainless steel plate with two parallel optical windows clamped
over the slot to form a sealed chamber. In order to meet the conditions
for a direct solution of Fick's law for the case of free diffusion it is
necessary that the channel be of uniform cross section.
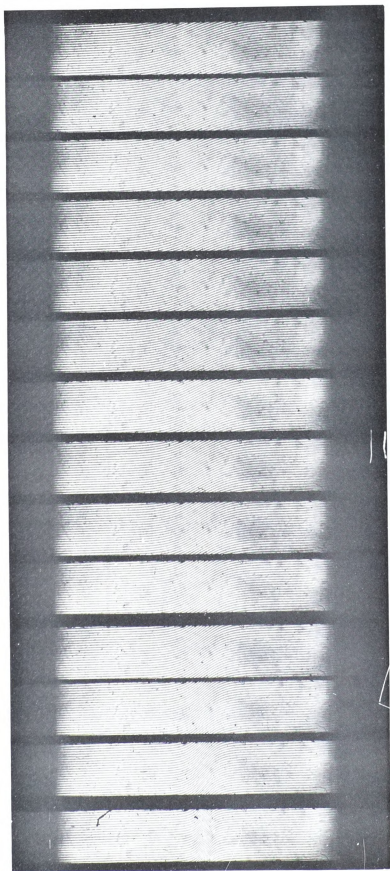
Figure 9. Set of Photographs Taken During Diffusion Run. (Experimental Run No. A-6).

Solution Reservoirs

Filling
Syringe

Valve 2

Valve 1

Cell
Window

Cell
Body

Valve 4

Valve 3

Boundary
Sharpening
Slits

Siphon

Valve 5
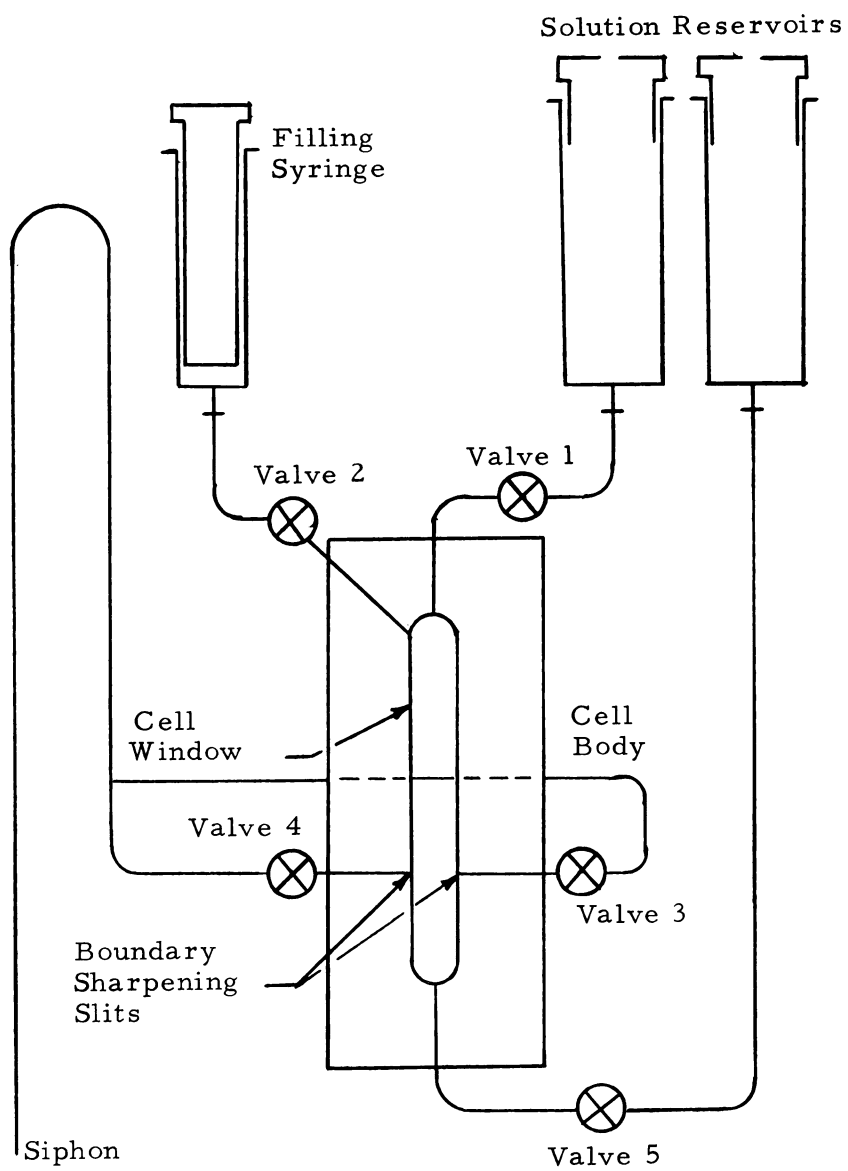
Figure 10. Diagram of Diffusion Cell.
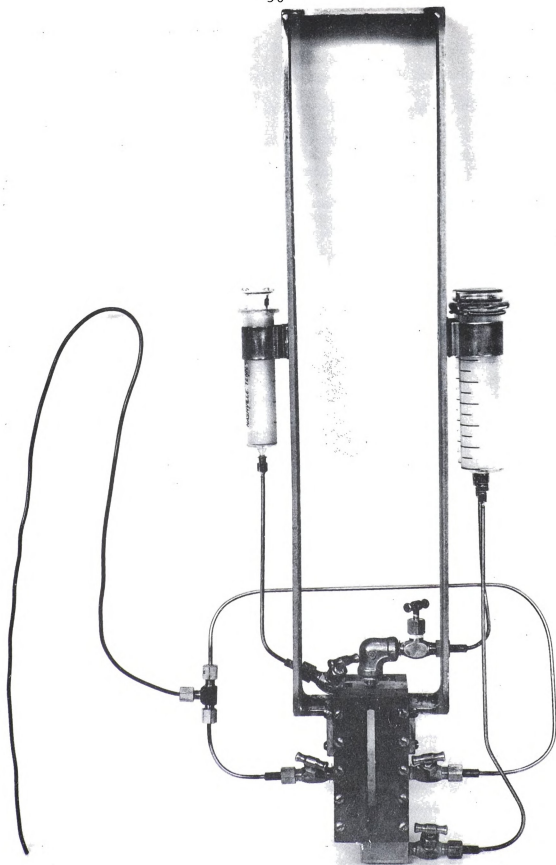
Figure 11. Photograph of Diffusion Cell for Measurement of Diffusion Coefficients

The boundary between two solutions of slightly different concentration was formed by the flowing boundary technique[7,33] by which the interface between the layers of liquid is formed by flowing the two liquids simultaneously through two fine horizontal slits in the cell wall. The denser solution is introduced at the bottom and the lighter solution at the top to prevent convection due to a density gradient.

The interferometer is so constructed that the fringe pattern can be observed by eye through a telescope or photographed by a camera. (See Figure 8) Thus it is possible to obtain a plot of refractive index versus distance at a given time interval. This information then allows us to calculate the diffusion coefficient. (See Appendix 1)

Procedure for Experimental Run of Diffusiometer

1) Two aqueous polyelectrolyte solutions of different concentration are prepared. In the case of polymethacrylic acid the desired degree of neutralization is obtained by addition of a known amount of sodium hydroxide.

2) The diffusion cell is clamped in a rack outside of the water bath with all valves closed.

3) Reservoir B (Figure 10) is filled with the more concentrated of the two solutions. Valves 5 and 1 are opened to allow the liquid to flow into the cell to approximately 3/4 inch above the exit slits. Valves 1 and 3 are then closed.

4) Valves 4 and 2 are opened and the exit line is filled with liquid by forcing the liquid out the exit with the syringe connected to valve 2. Care must be taken so that the liquid level does not drop below the slits.

5) Additional solution is allowed to flow into the cell as in step 3. This time the liquid is forced through valve 3 into the exit line. In order to assure complete removal of all air in the exit line this step must be repeated several times until the liquid will siphon out by itself. At this point the liquid level should be 1/8 inch above the slits. All valves are then closed and reservoir B is refilled.

6) The syringe above valve 2 is filled with the less dense solution and valve 1 is opened. Valve 2 is opened slightly and the solution is allowed to trickle down the wall of the cell until the cell is full and a small amount of solution appears in reservoir A. Reservoir A is then filled and valves 2 and 1 are closed.

7) The cell is placed into position on the cell hanger in the constant temperature water bath of the interferometer. Valves 1 and 5 are opened slightly until the rate of flow from the exit line is about 5-6 drops per minute. Then valve 4 is opened until the flow rate from the exit line is doubled (10-12 drops per minute).

8) The formation of the boundary can be observed through the telescope and when a satisfactory boundary is formed all the valves are closed, first closing valves 3 and 4 and then valves 1 and 5.

9) The mirror reflecting the image into the telescope is then removed so that the interference fringe pattern can be photographed by the camera.

10) A series of exposures are taken at a set time interval. A reproduction of a photographic plate appears in Figure 9.

11) After a run is completed, the cell is removed from the water bath, rinsed with acetone and dried by drawing air through the cell with an aspirator.

Calculation of Diffusion Coefficient

It is possible to apply Fick's second law, equation (1), to the diffusion in the cell described in Figure 10.   In order to solve Fick's second law

$$\frac{\partial^2 c}{\partial x^2} = \frac{1}{D} \frac{\partial c}{\partial t} \tag{1}$$

for the present case the following boundary conditions must be used:

Case I   (x > 0)   i) $x \rightarrow \infty$ $t \geq 0$ $c = c_1$
                    ii) $t = 0$ $c = c_1$ $\infty > x > 0$
                    iii) $x = 0$ $c = (c_1 + c_2)/2$ $t \geq 0$

Case II   (x < 0)   iv) $x \rightarrow -\infty$ $t \geq 0$ $c = c_2$
                    v) $t = 0$ $c = c_2$ $0 > x > -\infty$
                    vi) $x = 0$ $c = (c_1 + c_2/2$ $t \geq 0$

where x is defined in Figure 12.
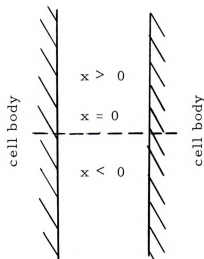
Figure 12.   Diffusion Cell Coordinates.

In order to solve equation (1) with the given boundary conditions it is necessary to assume that D is constant or is linear with c and the diffusion gradient has the properties of normal distribution curves. These assumptions are valid if c_1 and c_2 are nearly equal.

The solution to equation (1) may be obtained with Laplace transforms. The resulting solution is

$$\frac{c - c_o}{c_2 - c_1} = \frac{1}{2} \, \text{erf.} \left(\frac{x}{\sqrt{4Dt}} \right) \qquad (38)$$

for both Case I (x > 0) and Case II (x < 0). c_o is the concentration at the zero position in the cell and is equal to $\frac{1}{2} (c_1 + c_2)$.

For small differences in concentration, the refractive index, n, may be assumed proportional to the concentration,[50] and n can be substituted for c in equation (38) to obtain:

$$\frac{n - n_o}{n_2 - n_1} = \frac{1}{2} \, \text{erf.} \left(\frac{x}{\sqrt{4Dt}} \right) \quad . \qquad (39)$$

The fringe pattern obtained from the interferometer is a plot of the refractive index versus distance in the diffusion cell. The distances are magnified by the camera by a factor M.

A representation of the fringe pattern is given in Figure 13. In traversing from point A to point B, the total number of fringes crossed will be the number of fringes displaced by the difference in refractive index between the solutions at point A and B. Each fringe will correspond to a change in refractive index by an amount Δn.
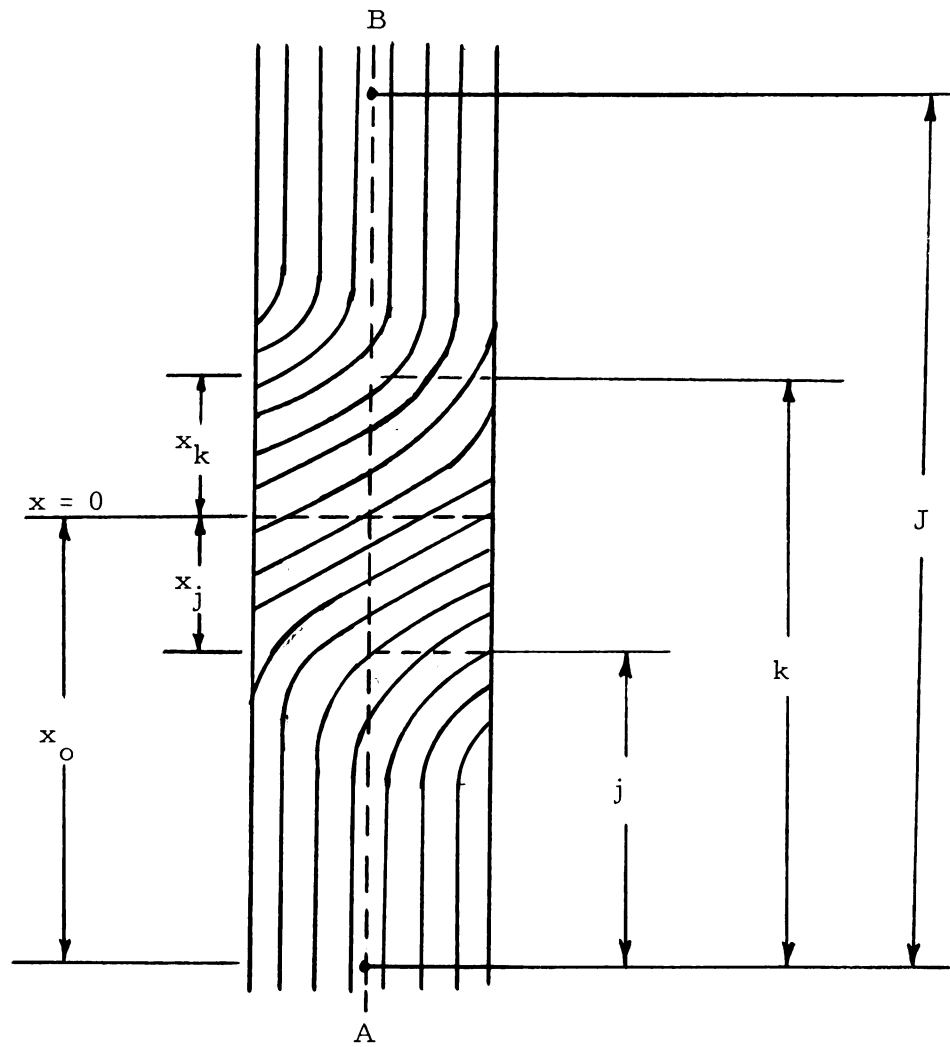
Figure 13. Fringe Pattern.

Let J be the total number of fringes and let k be the local fringe number in the top half of the cell and j the local fringe number in the bottom half. x_j and x_k are the measured distances corresponding to fringes j and k respectively.

Therefore, where x > 0

$$\frac{n - n_o}{n_2 - n_1} = \frac{k - \frac{1}{2}J}{J} = \frac{2k - J}{2J}$$

and equation (39) becomes

$$\frac{x_k}{\sqrt{4Dt}} = \text{erf}^{-1}\left(\frac{2k - J}{J}\right) \quad . \quad\quad (40)$$

Also, where x < 0

$$\frac{n - n_o}{n_2 - n_1} = \frac{J - 2j}{2J}$$

and

$$\frac{x_j}{\sqrt{4Dt}} = \text{erf}^{-1}\left(\frac{J - 2j}{J}\right) \quad . \quad\quad (41)$$

It is difficult to determine the midpoint of the diffusion; however, the distance, $x_k + x_j$, is easily determined by difference measurements. Therefore

$$\frac{x_j}{\sqrt{4Dt}} + \frac{x_k}{\sqrt{4Dt}} = \text{erf}^{-1}\left(\frac{J - 2j}{J}\right) + \text{erf}^{-1}\left(\frac{2k - J}{J}\right) \quad . \quad (42)$$

The measurements taken from the photographic plate are different from the cell distances because of the magnification by the camera lens. The image is magnified by a factor, M. Therefore,

$$\frac{x_j + x_k}{\sqrt{4Dt}} = \frac{x_j' + x_k'}{M\sqrt{4Dt}}$$

where x_j' and x_k' are distances on the photographic plate. Hence,

$$Dt = \frac{1}{4M^2} \left[\frac{x_j' + x_k'}{erf^{-1}\left(\frac{J-2j}{J}\right) + erf^{-1}\left(\frac{2k-J}{J}\right)} \right]^2 \quad (43)$$

The value

$$\left[\frac{x_j' + x_k'}{erf^{-1}\left(\frac{J-2j}{J}\right) + erf^{-1}\left(\frac{2k-J}{J}\right)} \right]^2$$

is obtained for several j's and k's for each exposure and averaged. The averages for several exposures are plotted versus exposure time. The slope of the resulting line is determined and thus,

$$D = \frac{slope}{4M^2} \quad (44)$$

The value for M was determined to be 1.923.[2] The calculated diffusion coefficient is assumed to be equal to the mutual diffusivity at the average concentration of the two solutions.

An optical comparator made from a Gaertner microscope was used to measure the distances on the photographic plate. The average deviation for the measurement of diffusivities by the Mach-Zehnder interferometer was determined to be 0.5%.[2]

Couette Apparatus

The electrical anisotropy effect was measured in a Couette apparatus. The Couette apparatus produces steady flow conditions with a constant velocity gradient perpendicular to the direction of motion in solutions which are in the annular gap between two concentric cylinders.

The apparatus was constructed according to the description given by Heckman[17] and several other investigators.[20,21,49] The principal features of the apparatus are shown in Figure 14. It consists essentially of a rotating outside cylinder (rotor) and a stationary inner cylinder (stator) with a narrow gap between the two cylinders. The gap width of the apparatus, which was constructed for these measurements, was approximately 0.05 cm.

Silver electrodes were imbedded in the surface of the stator to allow the measurement of the conductivity of the solution in the gap between the rotor and the stator. The electrodes were insulated from each other and from the brass cylinder by a thin layer of epoxy resin which covers the stator. A thin telfon lining was installed in the rotor to prevent conduction along the rotor wall.

The stator and the rotor were maintained at a constant temper-ature of 25°C by circulating cooiling water from an Arthur H. Thomas Co. constant temperature bath. The rotor was driven by a 1/3 H. P. Master direct current motor with a General Radio Co. variac speed control, the combination of these two pieces of equipment allow an infinitely variable speed drive. The rotational speed was determined
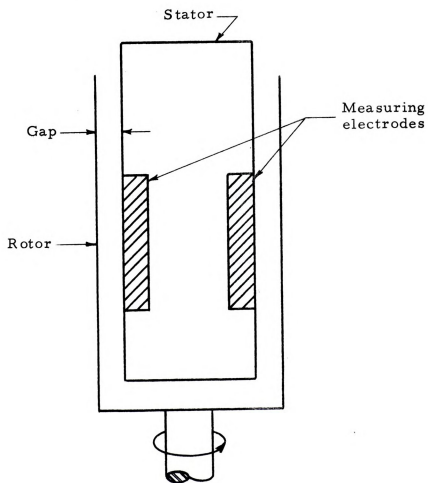
Figure 14.   Couette Apparatus (outline).

by a Hewlett Packard electronic counter which counts the electrical pulses generated by a magnetic pickup device activated by a series of gear teeth cut into the drive pulley. The counter converts the electrical pulses into a reading of R. P. M. Because of the required dimensions of the teeth in relation to the size of the magnetic pickup, it was only possible to fit 30 gear teeth into the drive pulley instead of the normal 60 teeth; therefore the number displayed by the electronic counter was one half the actual R. P. M. of the rotor.

The conductivities of the solutions were measured with an Industrial Instrument Inc. RC-18 conductivity bridge operating at 1,000 cycles/sec. The conductivity bridge is fitted with a cathode-ray oscillographic detector and the cell capacitance effects can be balanced out by means of a variable condenser in parallel with the variable resistance.

Figures 15 and 16 give a more detailed description of the apparatus. The rotor is mounted on three precision ball bearings to give stability and rotational accuracy. Two oil seals protect the ball bearings from the cooling water.

The stator is positioned by several bolts in the top. It is important that the stator is returned to the same position for each run.

The stator consists of a brass cylinder with a thin layer of epoxy resin. In order to apply the epoxy layer, a form was constructed of plexiglass around the brass cylinder. The epoxy resin was poured in between the plexiglass cylinder and the brass cylinder and allowed to harden. After the epoxy was cured in an oven for
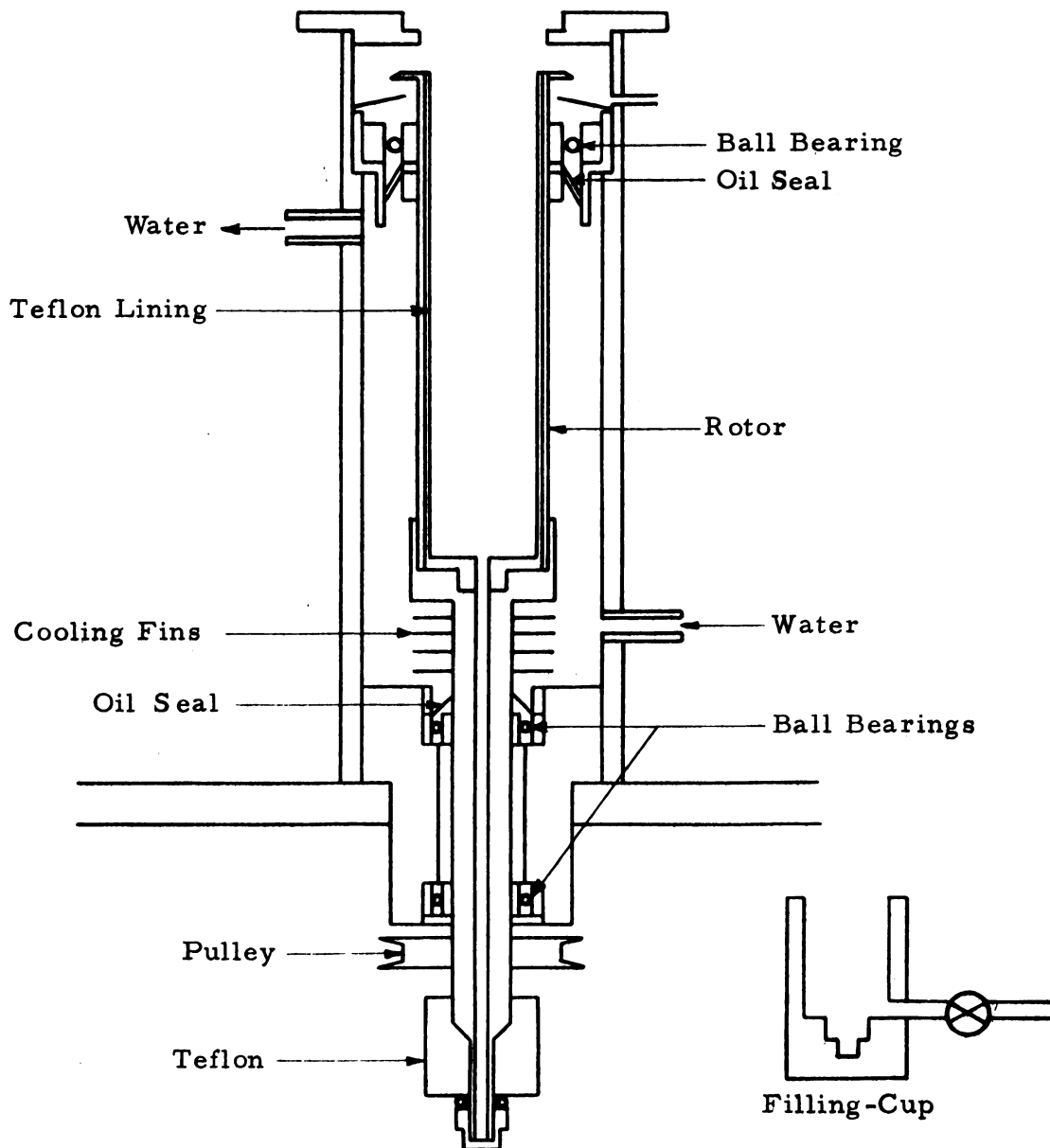
Figure 15. Couette Apparatus without Stator.
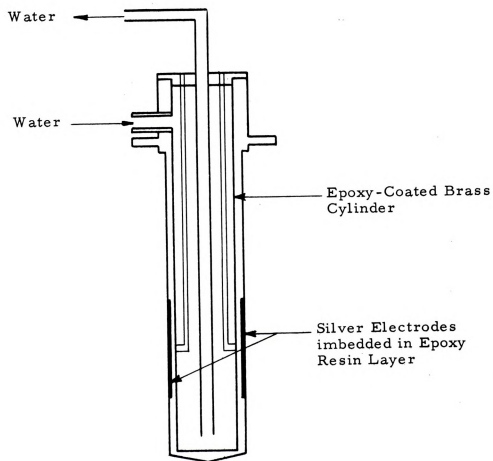
Figure 16. Stator for Couette Apparatus.

several hours, the plexiglass was cut off and epoxy was machined to the desired diameter.

The silver electrodes were placed into position before the epoxy was poured, so that the surface of the electrodes could be machined to the same diameter as the epoxy surface. This is necessary to assure steady uniform flow in the annular gap.

The polyelectrolyte solutions were introduced into the gap from below through a channel which was drilled through the rotor axle. The solutions were allowed to flow into the gap by gravity from a funnel connected by tygon tubing to a filling-cup. The filling-cup had a hexagonal nut fitted into a slot in the bottom. The rotor axle is threaded so that when the gap is filled with solution the nut can be screwed into place by turning the filling-cup.

Determination of the Size of the Polyion

The anisotropic behavior of the conductivity of charged particles in a conducting medium was calculated by Schwarz[42] (equation (36)). For the determination of the size of a rod shaped particle these functions are given in Figure 17 in the form of the normalized anisotropies $K(\sigma)$, for different abscissa scales, where K is equal to the relative change in conductivity divided by the value of the relative change for complete orientation of the charged particles.

The rotational diffusion constant D_r, was determined by comparison of the change of conductivity $A_y(q)$, measured in the Y direction (see Figure 3) as a function of the velocity gradient q, to the corresponding set of anisotropy curves calculated as functions of $\sigma = q/D_r$.

The experimental curve $A_y(q)$ was plotted with the arbitrary abscissa scale $M_a(\sec.^{-1}/cm.)$ and ordinate scale $M_o(fraction/cm.)$. The curve system in Figure 17 was projected upon the measured curves in such a way that one curve out of the system fits optimally to the measured values. The parameter P of this curve and the corresponding enlargement V (the length of the V-scale shown on Figure 17 measured in the plane of projection in decimeters) were determined. One obtains from these values the rotational diffusion constant

$$D_r(\sec^{-1}) = 10^{-3} M_a PV .$$

(45)

The value of D_r inserted into equation (25) gives 1, the length of the particles. Under ordinary conditions ($T = 300^{\circ}K$; $\eta_o = 0.01$ poise) one obtains approximately

$$1(cm) = 0.0022 \, (M_a PV)^{-1/3} . \tag{46}$$

From equation (46) and Figure 17 one observes that the length of the charged particles is directly related to the height of the relative change of conductivity curve.
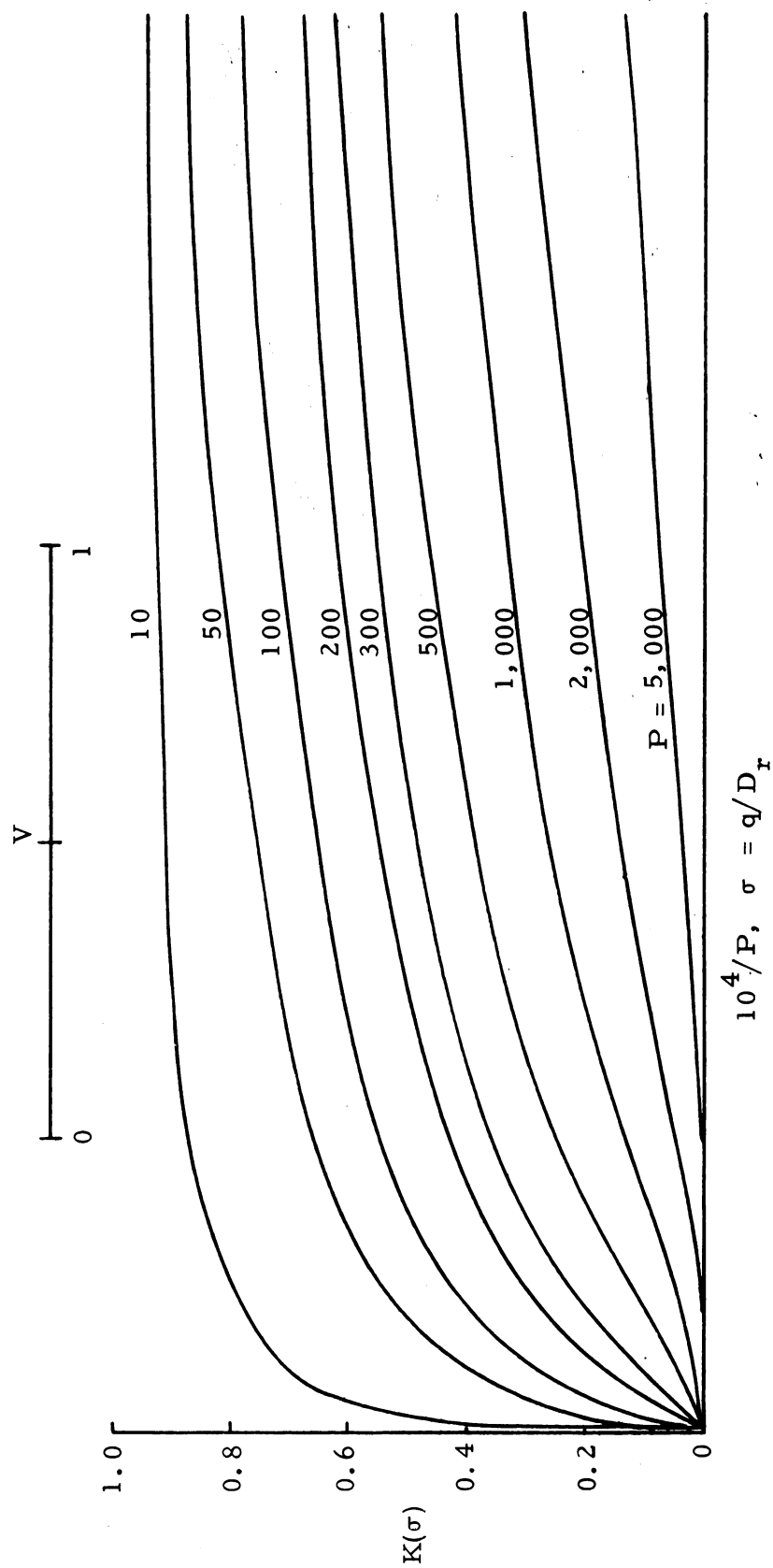
Figure 17. The Normalized Anisotropy $K(\sigma)$ for the Size Determination of Rod-Shaped Particles Based on Calculations by Schwarz[42] and Gotz.[14]

Synthesis of Potassium Polyphosphate

Potassium polyphosphate was prepared by heating primary potassium phosphate at $1200^{\circ}F$ for 24 hours. The polymerization is a condensation reaction and is described by the following equation:

$$n\ KH_2PO_4 \rightarrow (KPO_3)_n + n\ H_2O\ .$$

According to Van Wasser[6, 45] the polyphosphates are straight chain polymers and have the following structure:

$$-O-\overset{\overset{\displaystyle O^-K^+}{|}}{\underset{\underset{\displaystyle O}{\|}}{P}}-O-\overset{\overset{\displaystyle O^-K^+}{|}}{\underset{\underset{\displaystyle O}{\|}}{P}}-O-$$
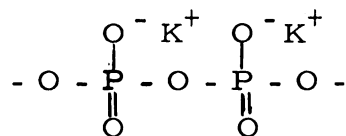
The polyphosphate chain undergoes hydrolysis quite rapidly in aqueous solution[46] and therefore the solutions must be prepared freshly for each run.

The molecular weight of the polyphosphate was determined from a viscosity correlation derived by Van Wasser[45] which relates the intrinsic viscosity of the polymer solutions to the average molecular weight, $\overline{M}_V$, T = 25 $^{\circ}C$.

$$[\eta]\ =\ K_i \overline{M}_V + K_o \tag{47}$$

where: $[\eta]$ = intrinsic vicosity

K_i = 1.25×10^{-5}

K_o = 0.085

A Cannon-Fenske[10] capillary tube viscosimeter was used to determine the viscosity of polyphosphate solutions of various concentrations of polymer dissolved in a 10% solution of tetramethyl-ammonium bromide. The intrinsic viscosity is obtained by plotting specific viscosity divided by concentration versus concentration and extrapolating to zero concentration. Thus,

$$[\eta] = \lim_{C \to 0} \frac{\eta_{sp}}{C}$$

According to Billmeyer,[3] $\eta_{sp} = (t - t_o)/t_o$, where t is the efflux time for a given volume of polymer solution and t_o is the corresponding efflux time for the solvent.

Figure 18 is the plot of η_{sp}/C versus C for the polyphosphate sample that was used in the diffusion experiments. When extrapolated to zero concentration the value for the intrinsic viscosity is equal to 8.0. Substituting $[\eta] = 8.0$ into equation (47), gives $\overline{M}_v = 640,000$.
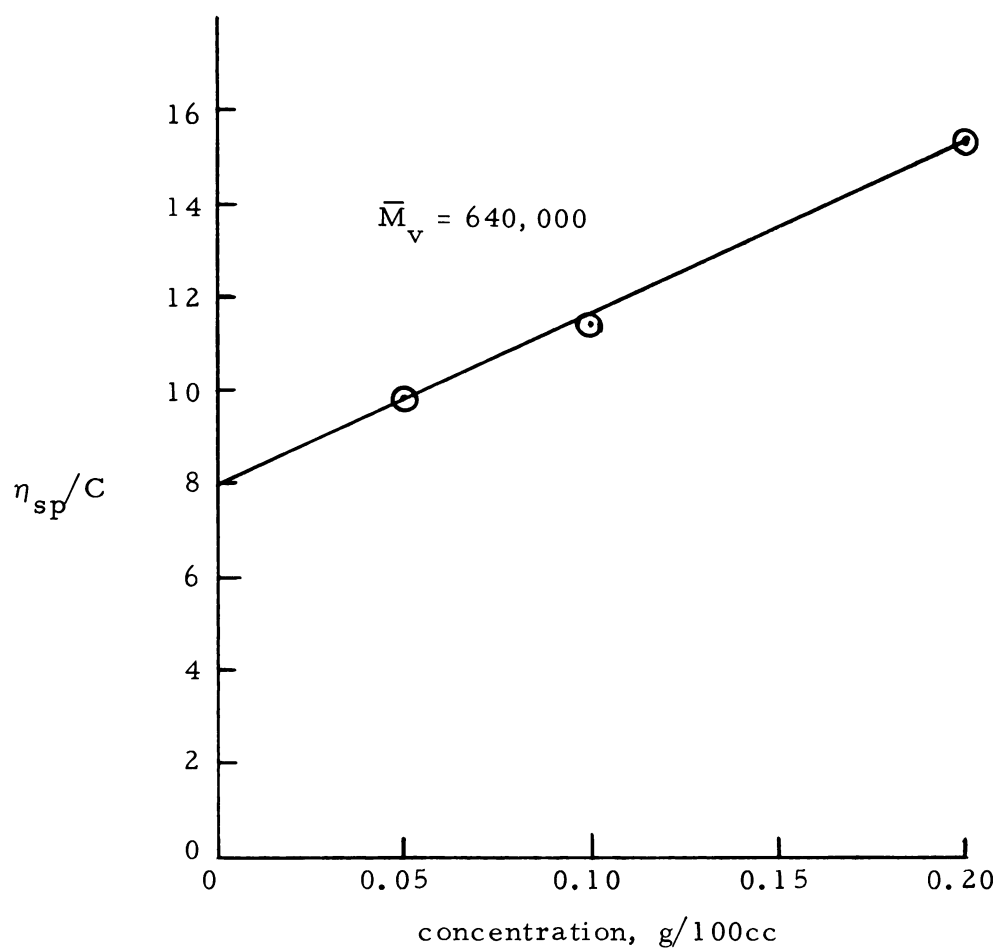
Figure 18. Plot of η_{sp}/C versus Concentration for Potassium Polyphosphate in 10% Solution of Tetramethylammonium Bromide.

Synthesis of Polymethacrylic Acid

Polymethacrylic acid was synthesized from the monomer methacrylic acid by a free radical type polymerization. The monomer, purchased from Eastman Chemicals, was first distilled under a vacuum to remove the inhibitor and then polymerized in a water-methanol solution using 0.5% benzoyl peroxide as the free radical initiator. The mixture was agitated by bubbling nitrogen through the solution and the temperature was maintained at $70^\circ C$ by immersing the rector flask in a constant temperature bath. The appearance of a cloudy and viscous solution indicated completion of the reaction. [48]

The swollen polymer was dissolved in methanol and precipitated with ether to remove the monomer and catalyst. This procedure was repeated several times to ensure the complete removal of monomer and catalyst.

The polymethacrylic acid was then redissolved in methanol and fractionally precipitated by the gradual addition of ether to obtain different molecular weights. The fractionation procedure used was essentially that proposed by Flory. [12] The fractions were dried in a vacuum at $110^\circ C$ for 48 hours and then ground to a fine powder.

The resulting polymer has the formula

$$\left(\begin{array}{c} CH_3 \\ | \\ -CH_2 - C - \\ | \\ C = 0 \\ | \\ OH \end{array} \right)_n$$
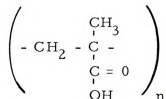
where n represents the degree of polymerization.

The molecular weights were determined by viscosity measurements of polymer solutions in 2N sodium hydroxide according to the procedure outlined by Katchalsky and Eisenberg.[25]

Figure 19 is a plot of η_{sp}/C versus C for the different polymer samples used in the experiments. By extrapolation to zero concentration, the intrinsic viscosity is obtained. The intrinsic viscosity for the polymer solutions is related to the degree of polymerization (DP) and molecular weight as given in Figure 20.[25]
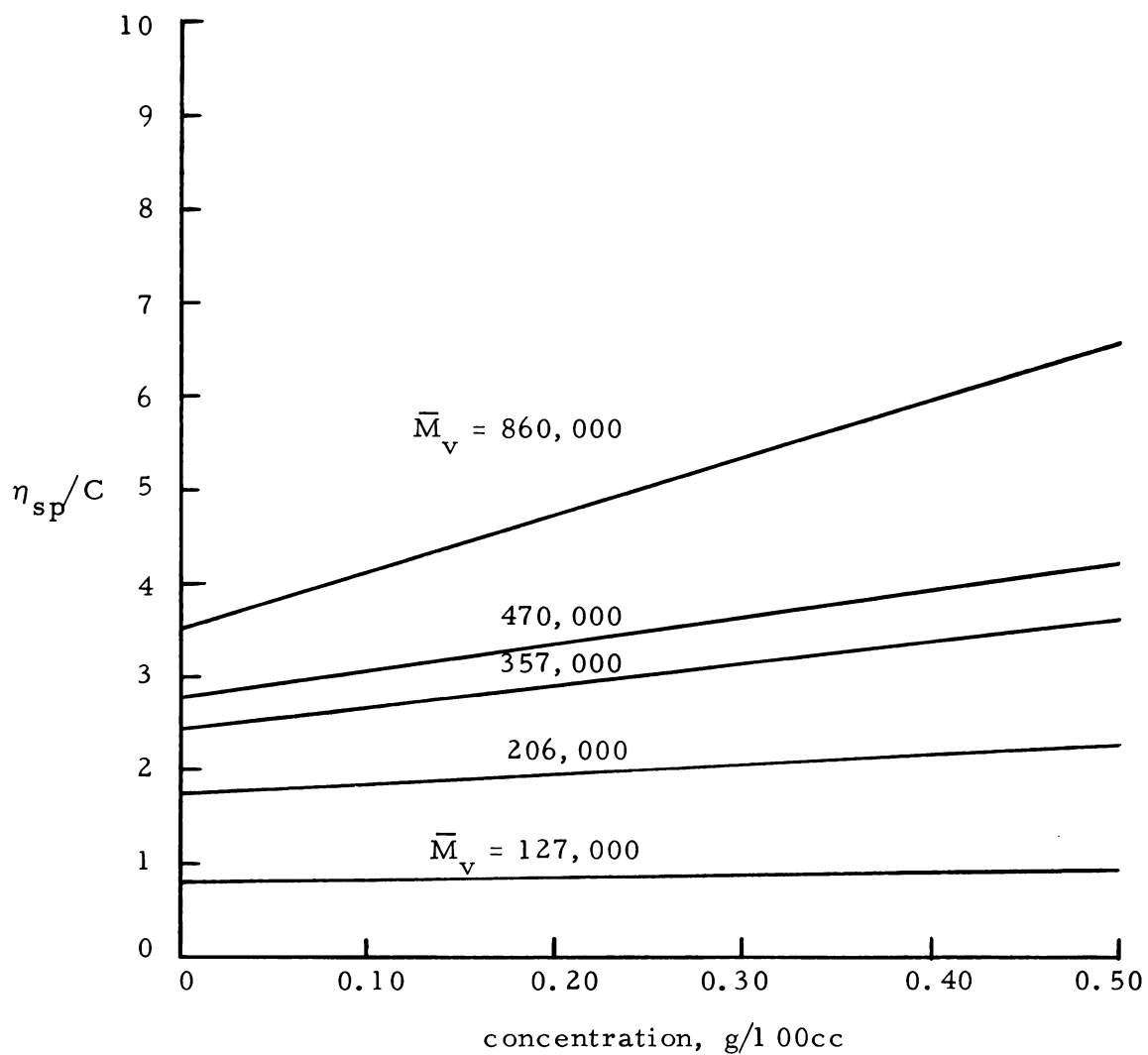
Figure 19. Plot of Reduced Viscosity versus Concentration for
Polymethacrylic Acid in 2N Sodium Hydroxide.
T = 30°C.
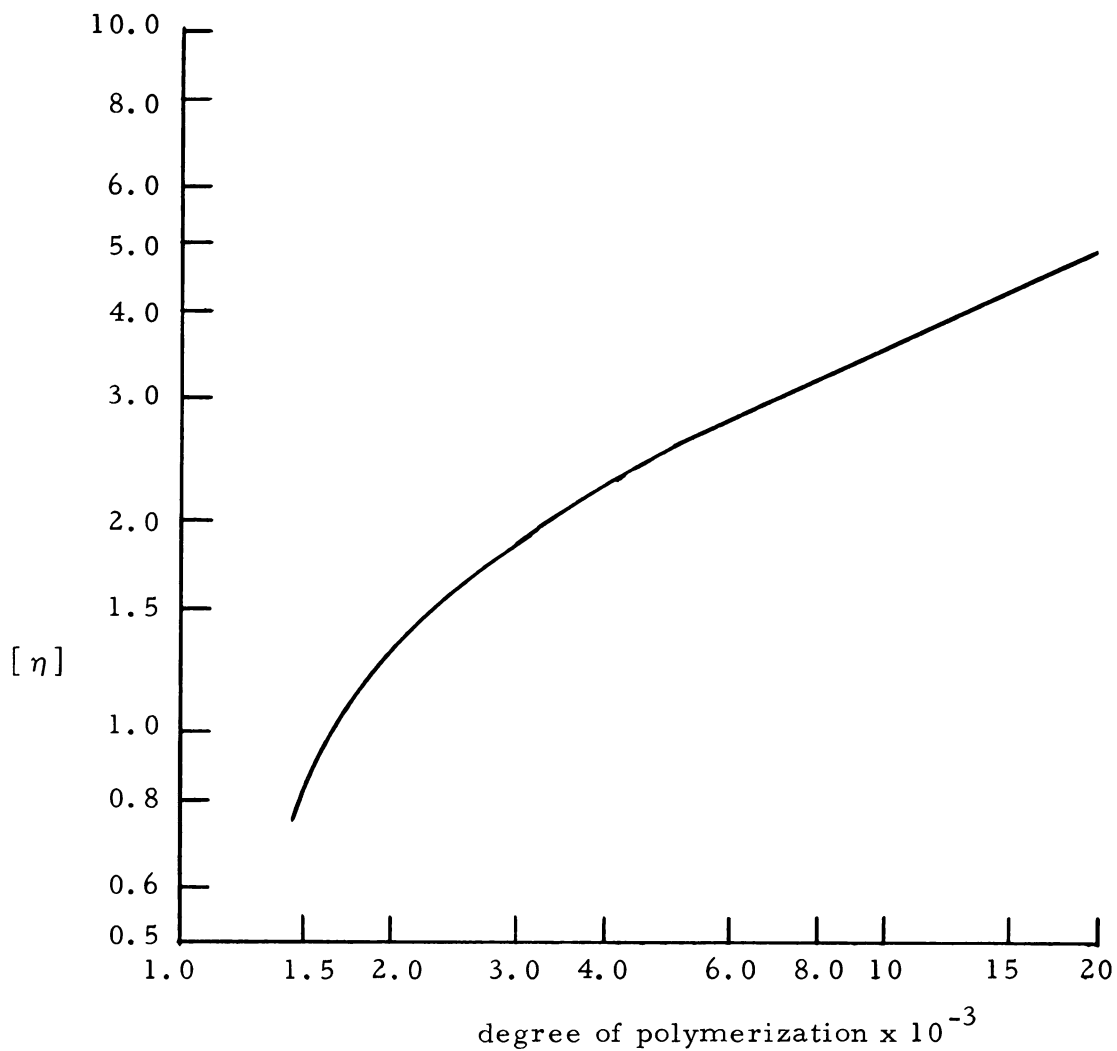
Figure 20. Plot of Intrinsic Viscosity versus Degree of Poly-
merization of Polymethacrylic Acid in 2N Sodium
Hydroxide. From Reference 25.

RESULTS AND DISCUSSION

The experimental results for the diffusion of polymethacrylic acid are tabulated in Appendix II along with viscosity measurements of the polymer solutions. Diffusion coefficients, D, were obtained as a function of the degree of neutralization, α, of the acid groups for different molecular weights and different average concentrations.

Figures 21 to 24 are plots of the diffusion coefficients of polymethacrylic acid. These plots show the dependence of D upon α for several different molecular weights and different average concentrations.

It can be seen that the molecular weight of the polymer has very little effect upon the plot of D versus α, but the curve is markedly effected by a change in the average concentration of the polymer solutions.

The initial increase of D is readily explained by the increase in the number of counterions, which according to equation (11)

$$D = \frac{kT}{\rho} \nu \left(\phi + \frac{\partial \phi}{\partial \ln n} \right) \tag{11}$$

and the theory of the Nernst potential should cause an increase in D. Beyond 10%, D decreases in all cases because of the increase in the hydrodynamic resistance of the polyion. From 0 - 10% neutralization the molecules are hypercoiled by intramolecular hydrogen bonds and their hydrodynamic resistance, ρ, is relatively small. Beyond 10% neutralization the molecules open up by virtue of the intramolecular electrostatic repulsion (equation 19), so that ρ
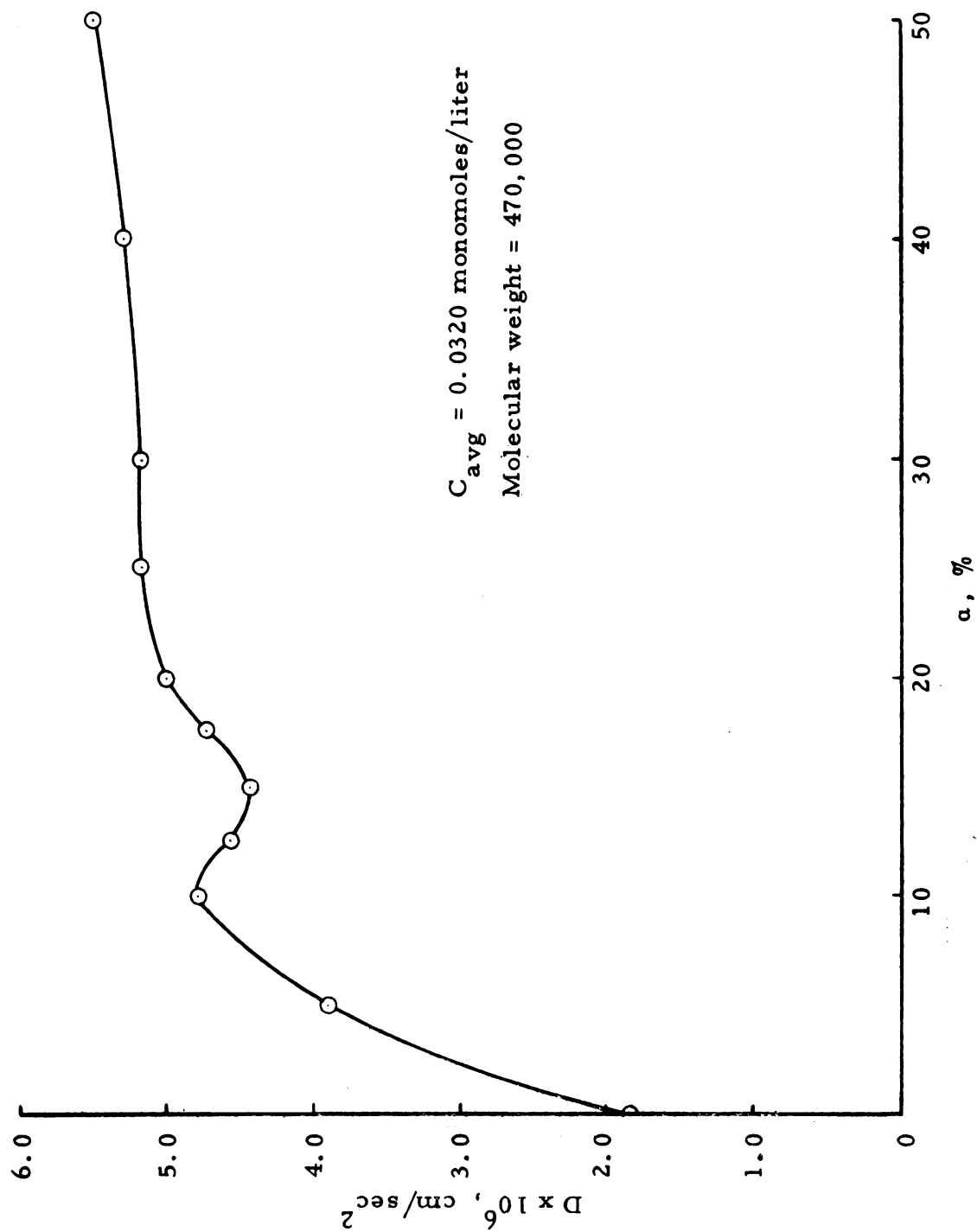
Figure 21. Plot of Diffusion Coefficient versus Degree of Neutralization for PMA at $C_{avg.}$ = 0.0320 Monomoles/Liter, Molecular Weight = 470,000.
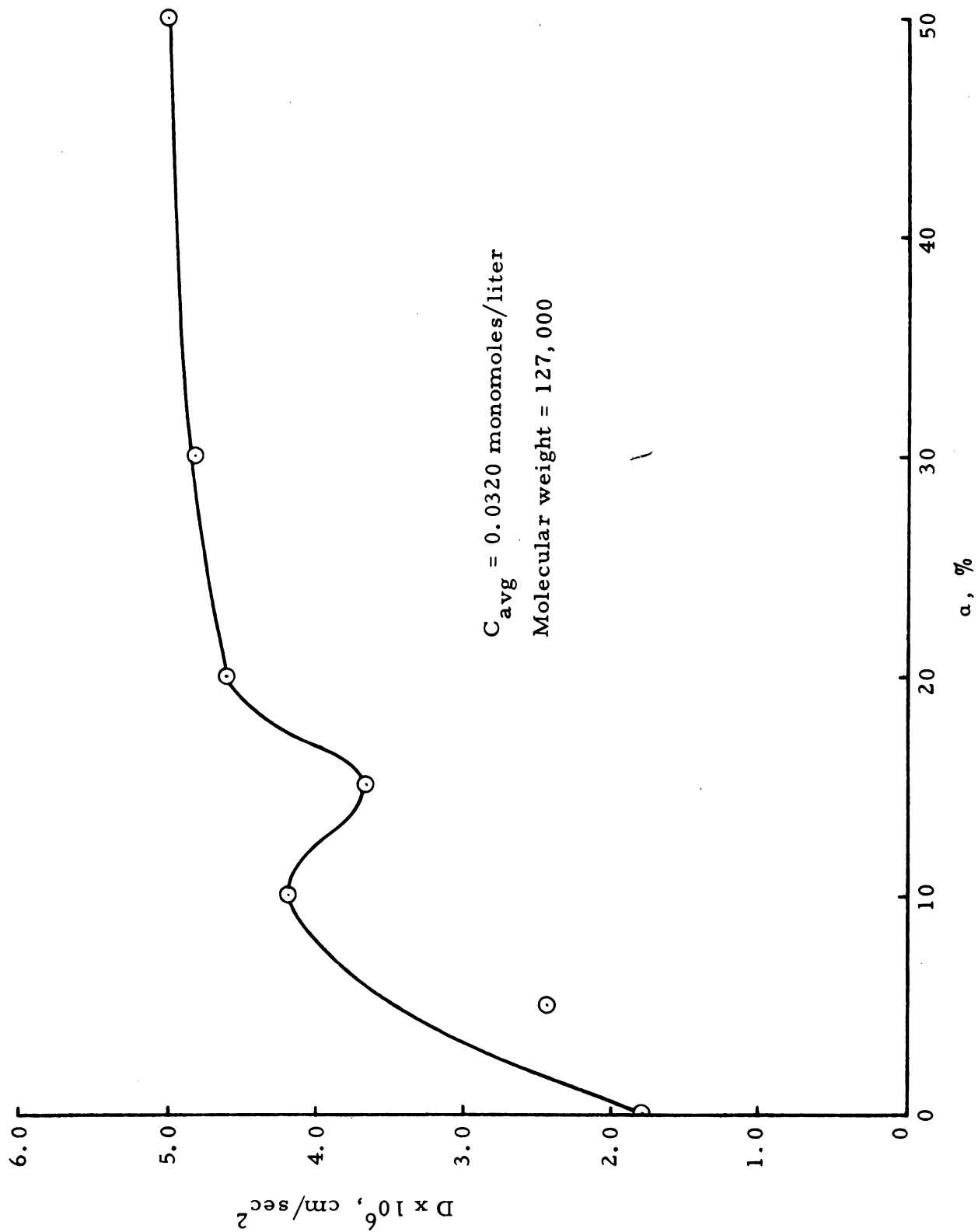
Figure 22. Plot of Diffusion Coefficient versus Degree of Neutralization at $C_{avg.} = 0.0320$ Monomoles/Liter, Molecular Weight = 127,000.
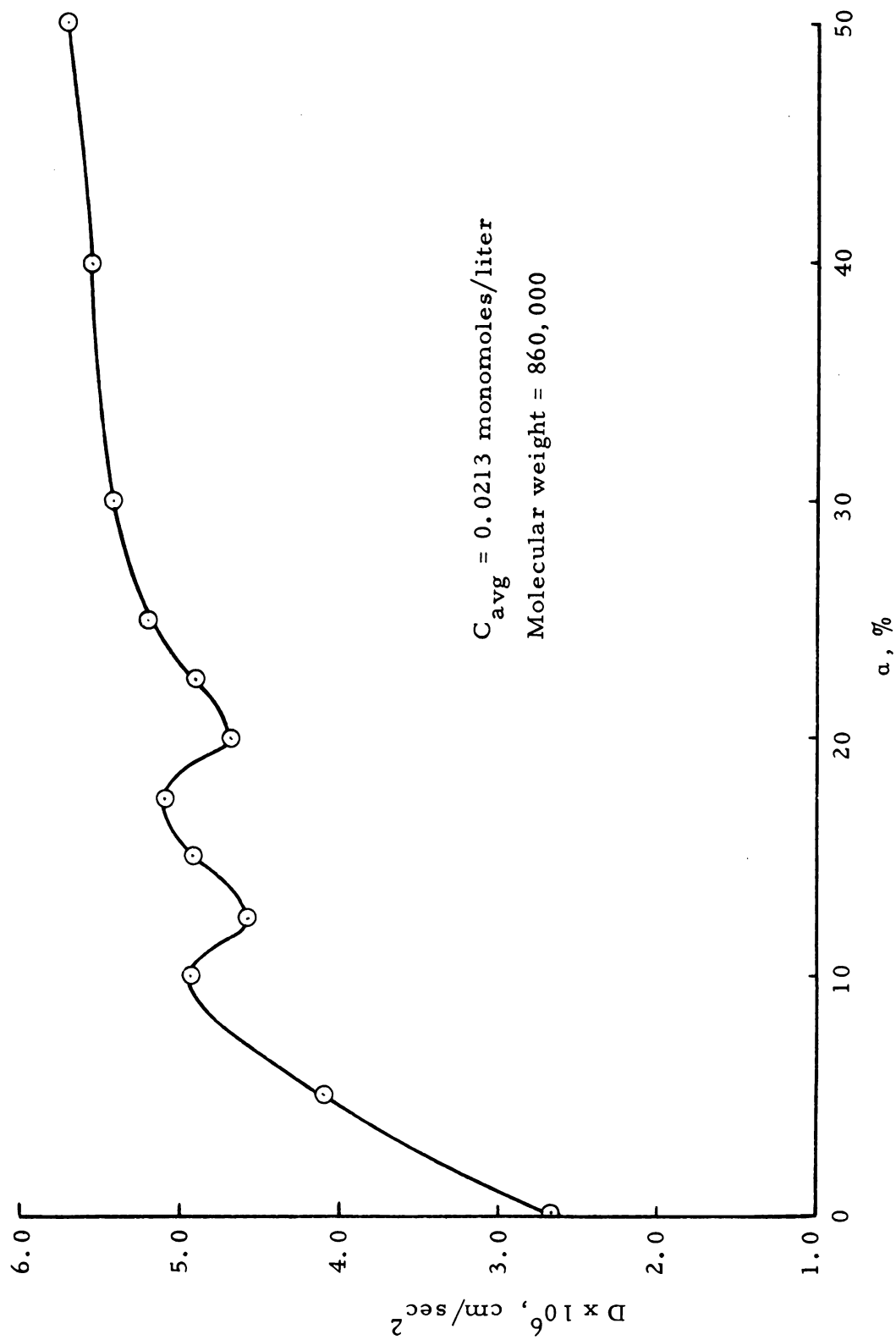
Figure 23. Plot of Diffusion Coefficient versus Degree of Neutralization at
C_{avg} = 0.0213 Monomoles/Liter, Molecular Weight = 860,000.
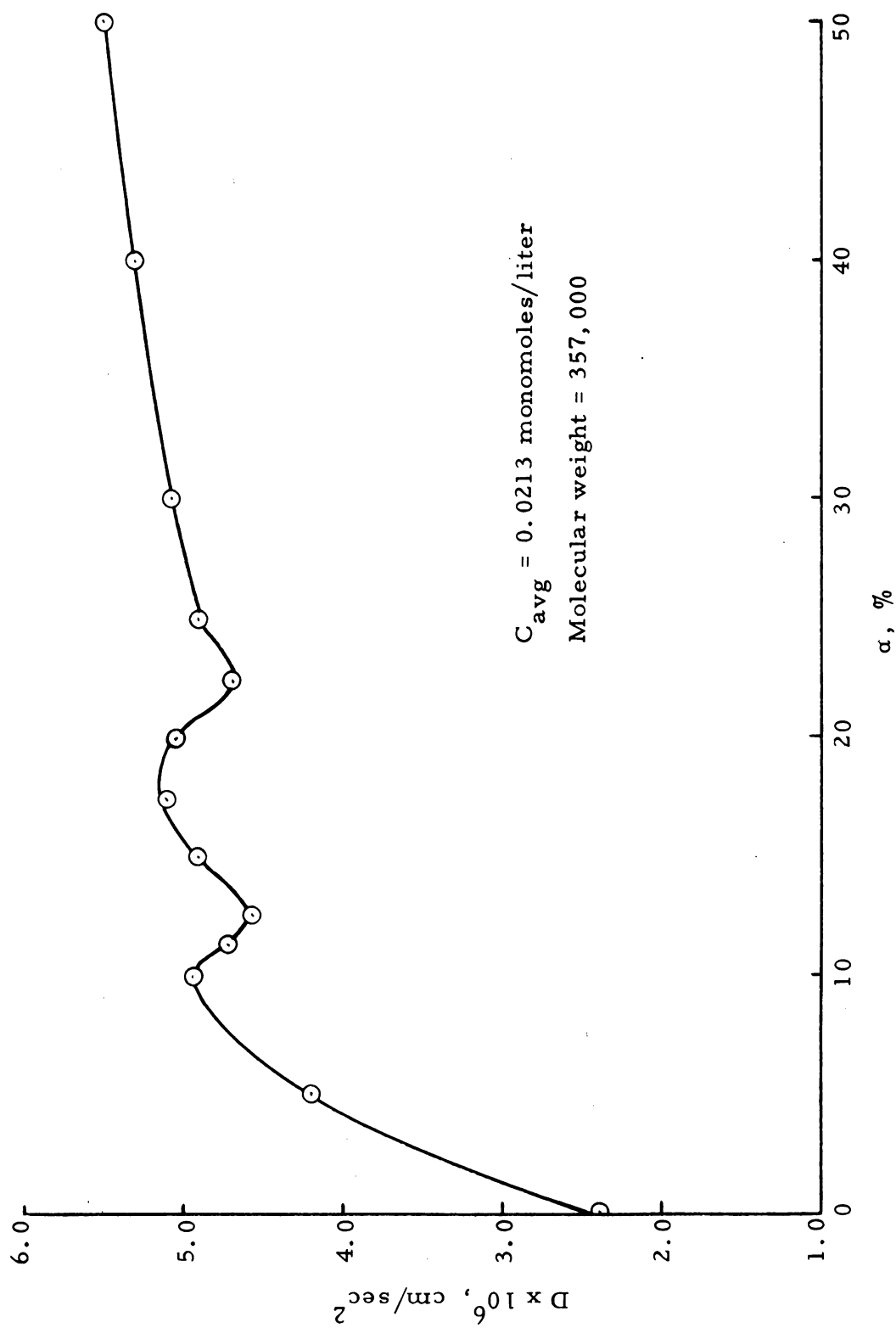
Figure 24. Plot of Diffusion Coefficient versus Degree of Neutralization at $C_{avg.} = 0.0213$ Monomoles/Liter, Molecular Weight = 357,000.

increases rather sharply. The increase in ρ, which is more rapid

than that in $\nu(\phi + \partial\phi/\partial \ln n)$ causes a decrease in D, as would

be expected from equation (11).

Kedem and Katchalsky[29] observed this same phenomenon, but

this investigation obtained a second decrease in D at lower concen-

trations. One can clearly see in Figures 23 and 24 that a two step

process is occurring in the uncoiling and opening of the polyion at

the lower concentration.

In order to verify that the decrease in D was due to a rapid

increase in the size of the polyion for both the depressions in D

versus a curves that are observed in Figures 23 and 24, it was

necessary to study the size of the polyion as a function of a by an

independent means. The electrical anisotropy effect gives an

approximate measure of the size of charged molecules in a conducting

medium.

The experimental results from the Couette apparatus for the

relative change of conductivity, $A = (K - K_o)/K_o$, as a function of

R.P.M. for different degrees of neutralization and concentration are

tabulated in Appendix IV and plotted in Figure 25 to 28.

As noted on page 46, the size of the polyion is proportional

to the cube root of the height of the relative change of conductivity

curve. Therefore a plot of the relative change of conductivity, A at

a particular R.P.M. versus a should give a qualitative picture of

the size dependence of the polyion upon the degree of neutralization.

Figures 29 and 30 are plots of A_{400} versus a for different

concentrations. Again it can be seen that there are two abrupt changes
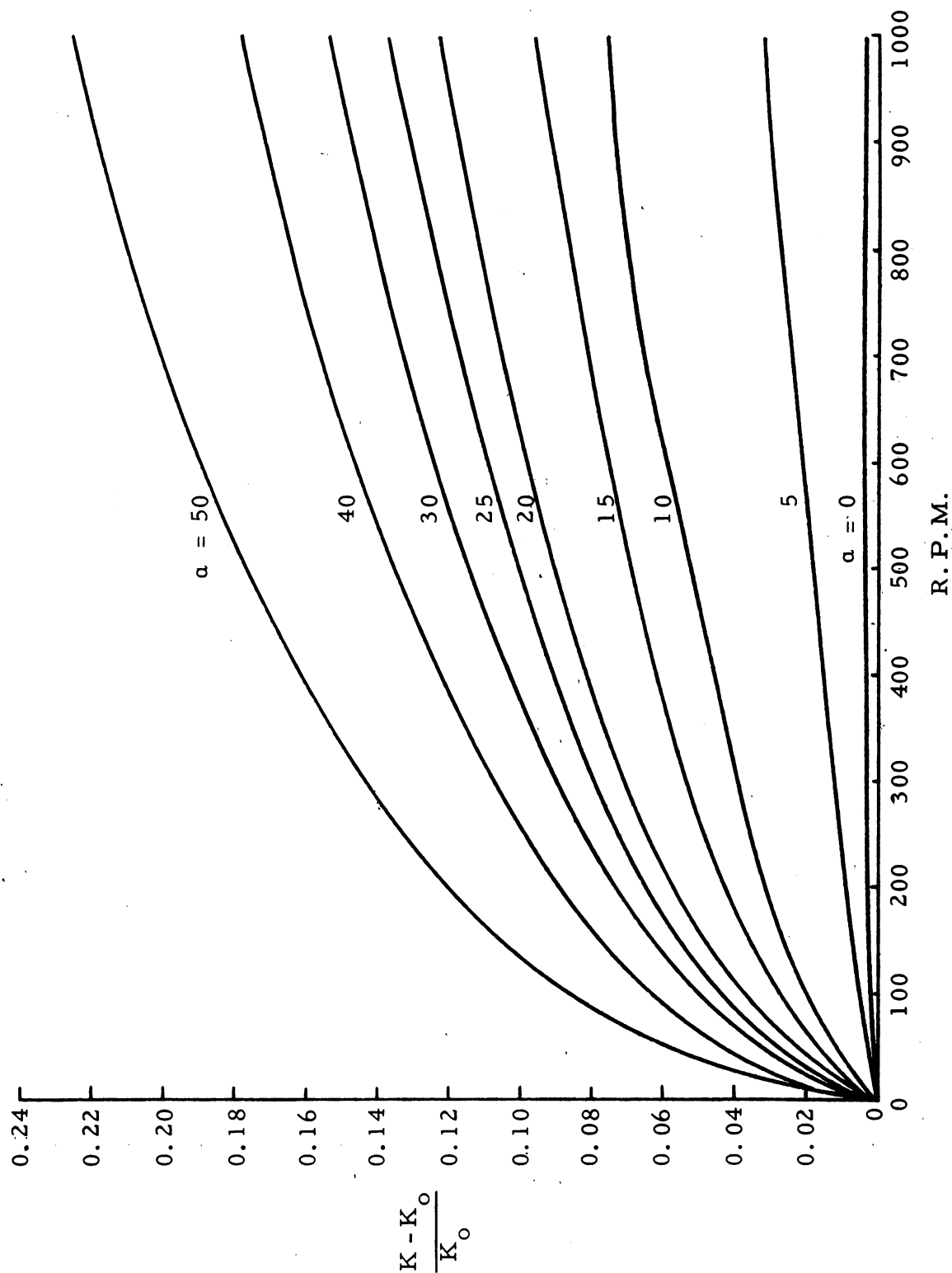
Figure 25. Plot of the Relative Change in Conductivity versus R.P.M. for PMA at 0.0058 monomoles/liter. Parameter α = Degree of Neutralization.
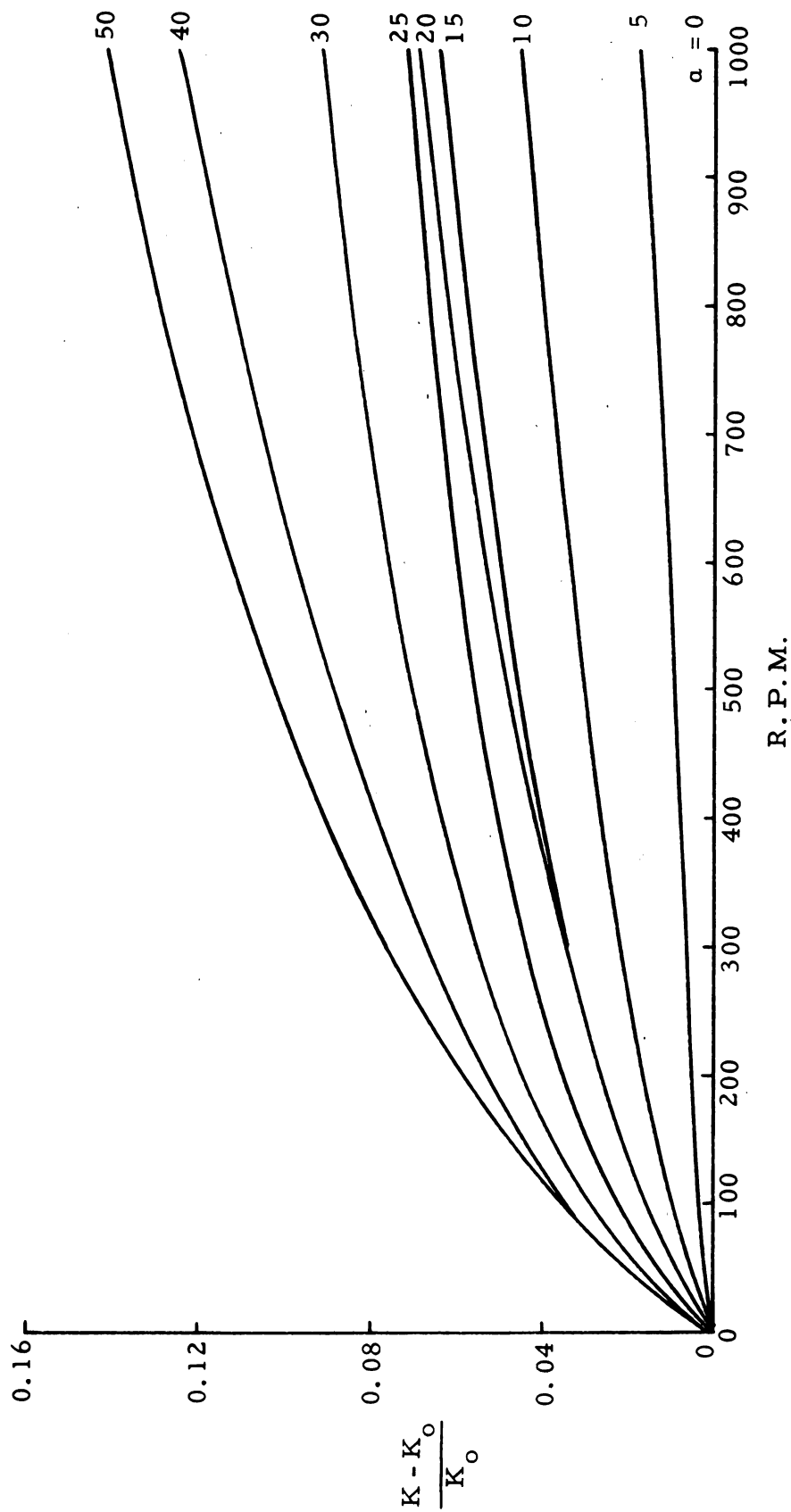
Figure 26. Plot of the Relative Change in Conductivity versus R. P. M. for PMA at 0.0116 monomoles/liter. Parameter α = Degree of Neutralization.
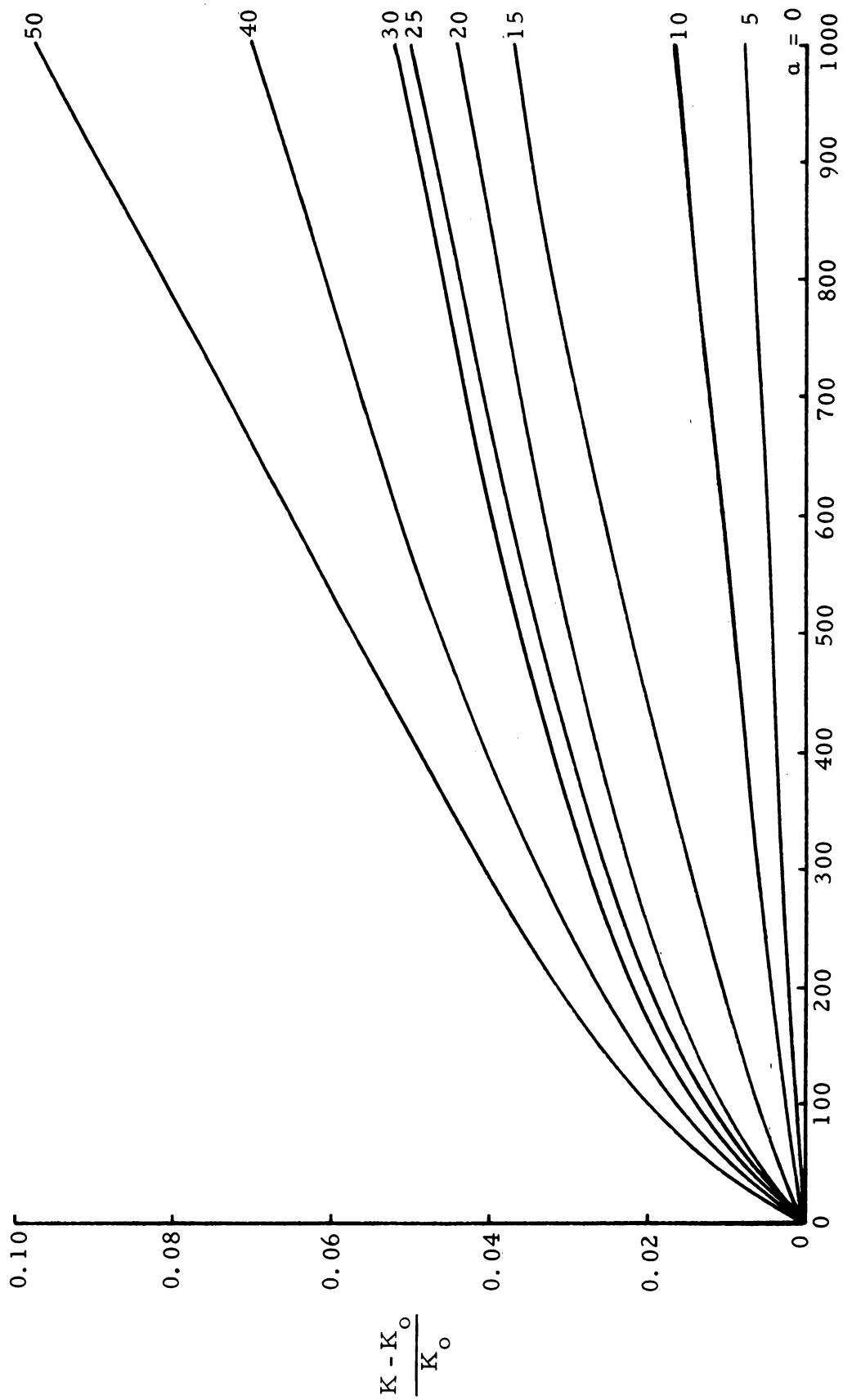
Figure 27. Plot of the Relative Change in Conductivity versus R. P. M. for PMA at 0.0213 monomoles/liter. Parameter α = Degree of Neutralization.
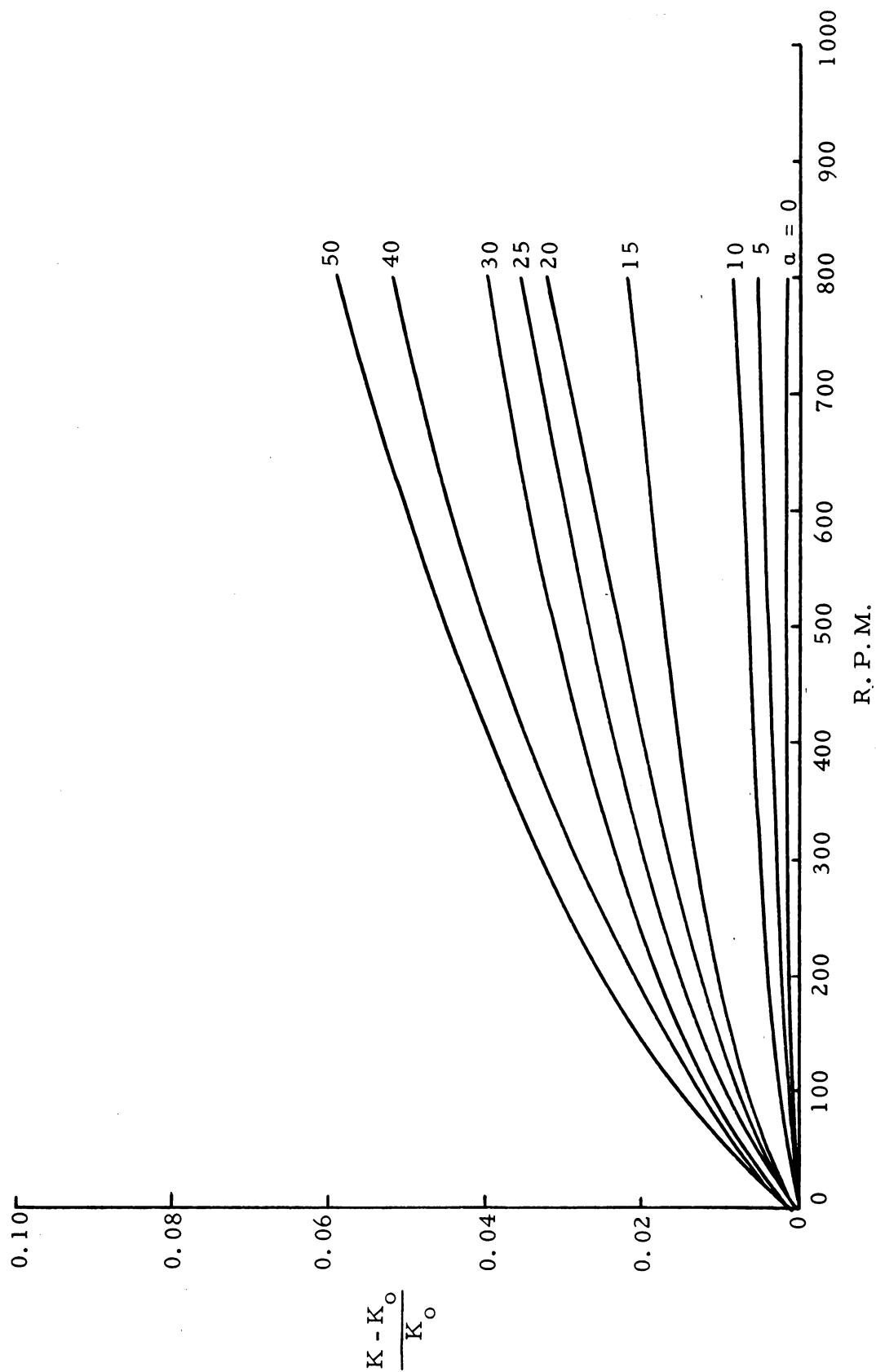
Figure 28. Plot of the Relative Change in Conductivity versus R. P. M. for PMA at 0.0291 monomoles/liter. Parameter α = Degree of Neutralization.
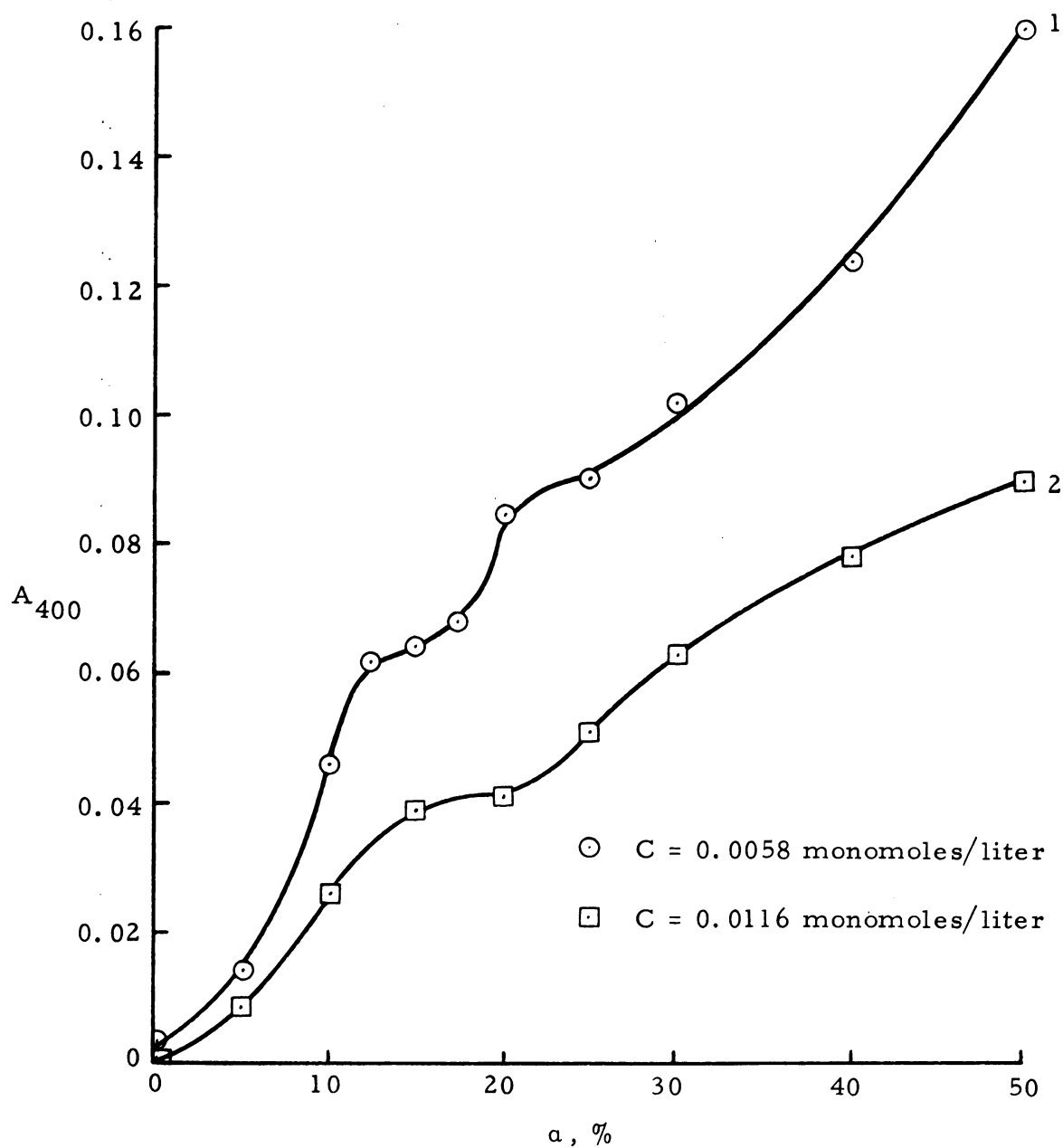
Figure 29. Plot of the Relative Change in Conductivity at 400 R. P. M. versus Degree of Neutralization. ① C = 0.0058 monomoles/liter. ② C = 0.0116 monomoles/liter. $\overline{M}_v$ = 206,000.
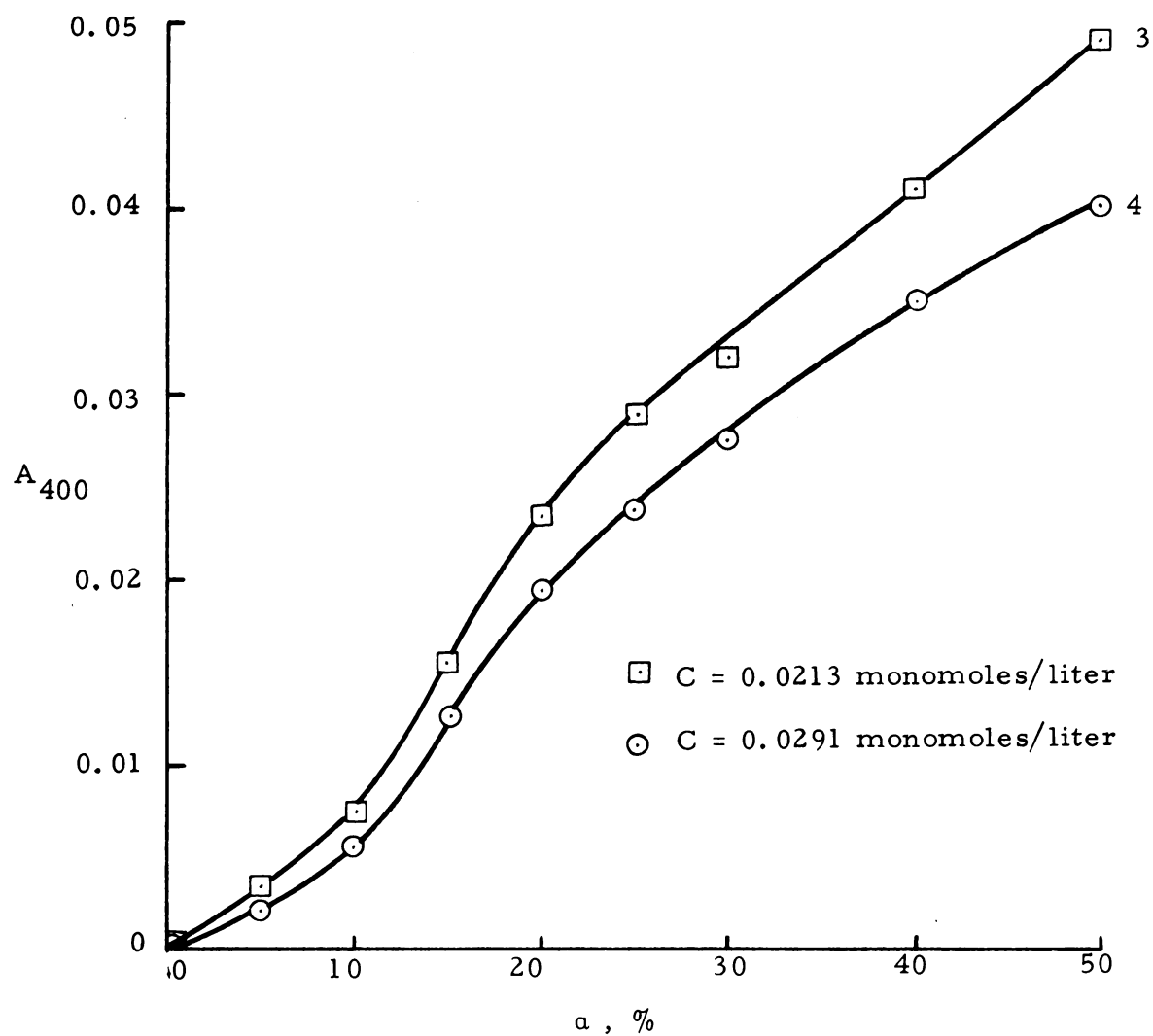
Figure 30. Plot of the Relative Change in Conductivity at 400 R. P. M. versus Degree of Neutralization. [3] C = 0.0213 monomoles/liter. (4) C = 0.0291 monomoles/liter. $\overline{M}_v$ = 206,000.

in the size of the polyion at the lower concentrations and only one abrupt change in the size of the polyion at the two higher concentrations. Also the abrupt changes in size occur at approximately the same values of α as do the depressions in the D versus α curves of Figures 21, 22, 23 and 24.

The data from the electrical anisotropy effect do indeed verify that the depressions in the D versus α curves are due to the sudden increase of the size of the polyion and indicates that a two step process is involved in the opening and uncoiling of the polyion.

The viscosity measurements are represented in Figures 31 to 34. The kinematic viscosity is plotted versus α for different concentrations and molecular weights corresponding to the solutions used in the diffusion measurement. Each curve indicates a rapid increase in viscosity between 10% and 30% neutralization. This increase in viscosity is assumed to be due to the opening of the coiled polymers.

Originally the increase in viscosity was attributed to electro-viscous effects, but a quantitative estimate showed that the increase is much greater than might be expected from the electroviscous behavior of the solutions.[24]

The curve in Figure 32 for the concentration of 0.0213 monomoles per liter has a rather steep slope between 10 and 15%, the slope then decreases until at 20% and then increases again to beyond 25%. Thus if the increase in viscosity is due to the opening of the polymer chain as assumed, then this curve also indicates a two step process in the opening and uncoiling of the polymer chain. The concentration of 0.0213 monomoles/liter is the same as the average concentration in Figures 23 and 24.
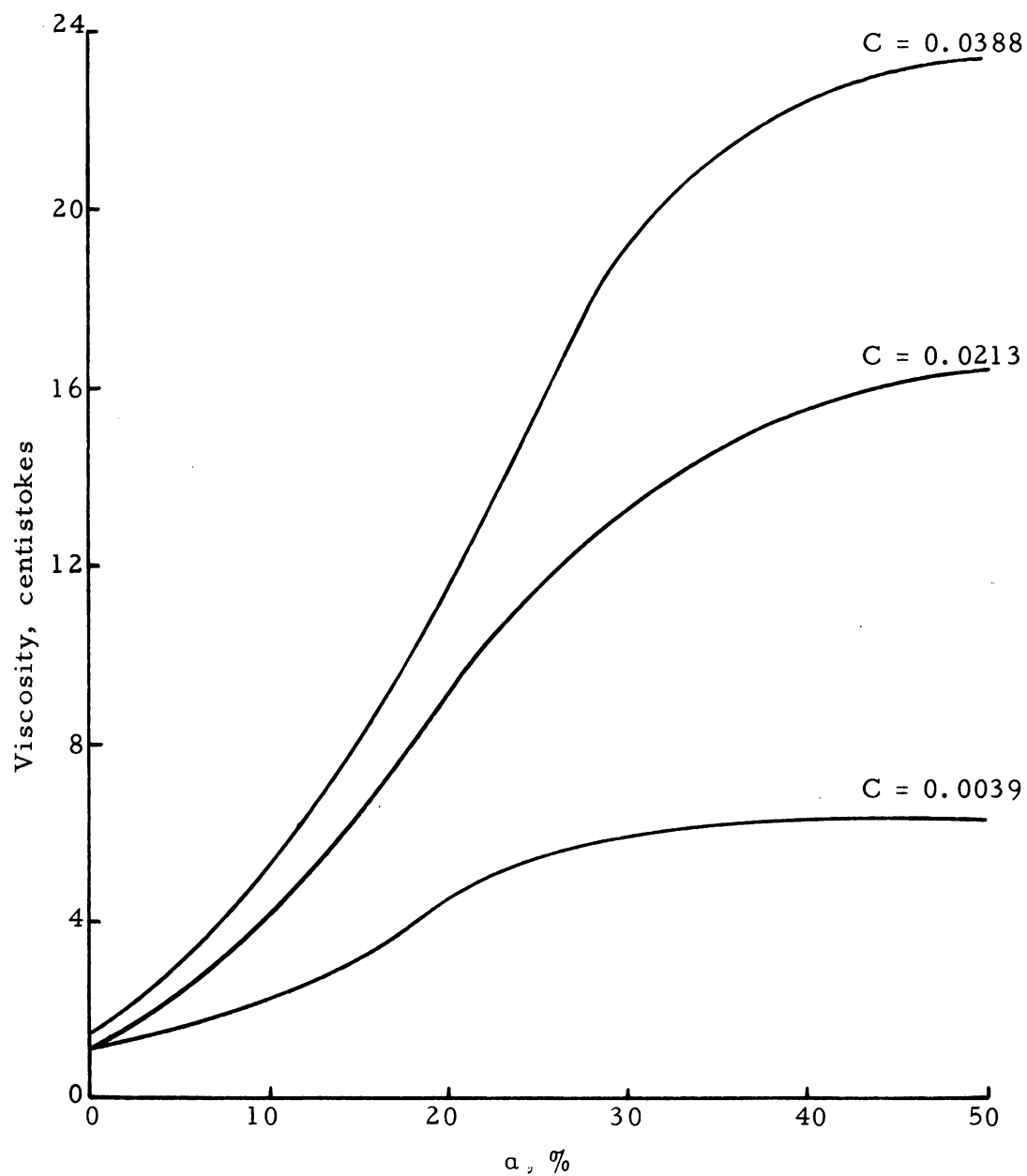
Figure 31. Plot of Apparent Viscosity versus Degree of
Neutralization for PMA Solutions, Molecular
Weight = 357, 000.
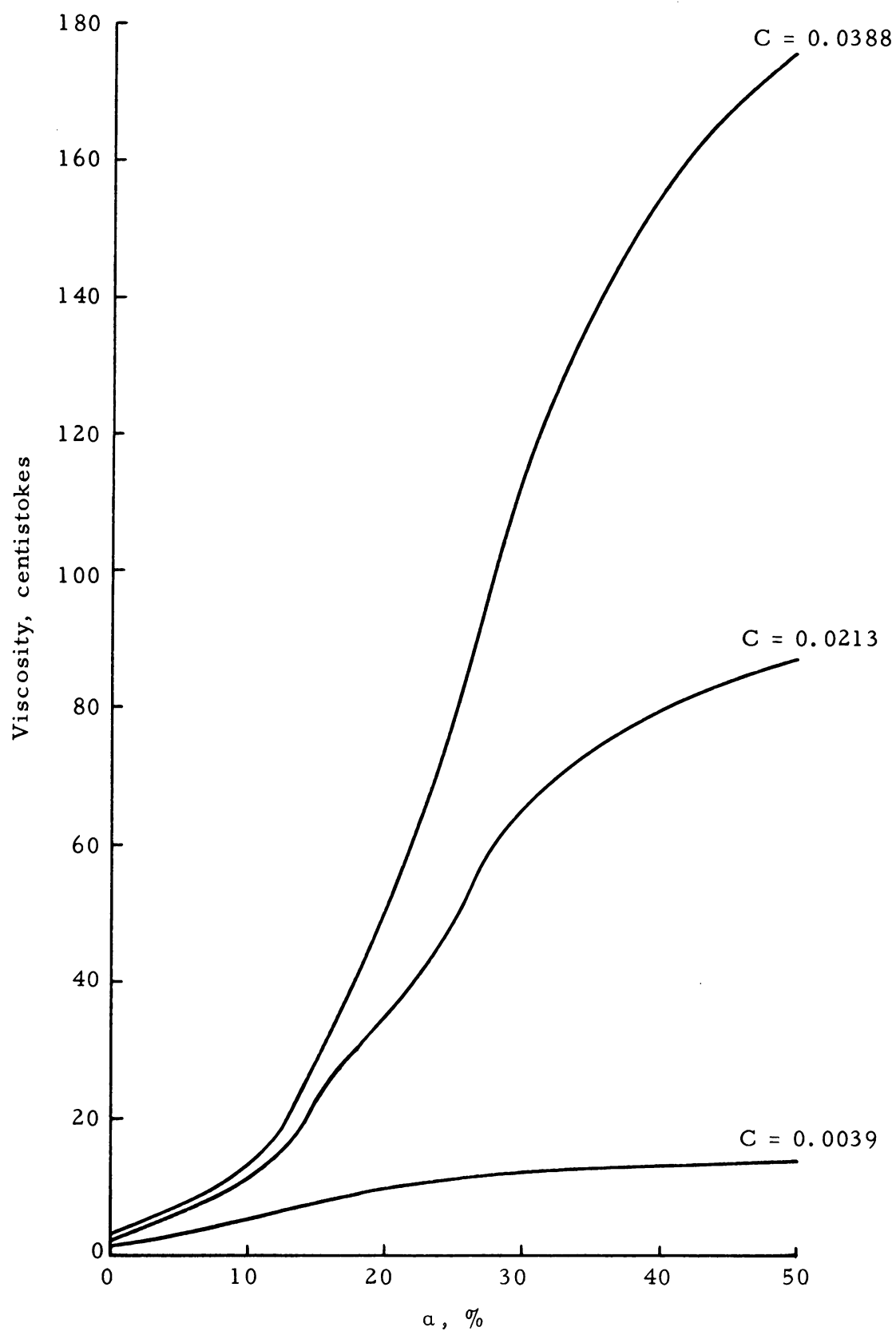
Figure 32. Plot of Apparent Viscosity versus Degree of
Neutralization for PMA Solutions. Molecular
Weight = 860,000.
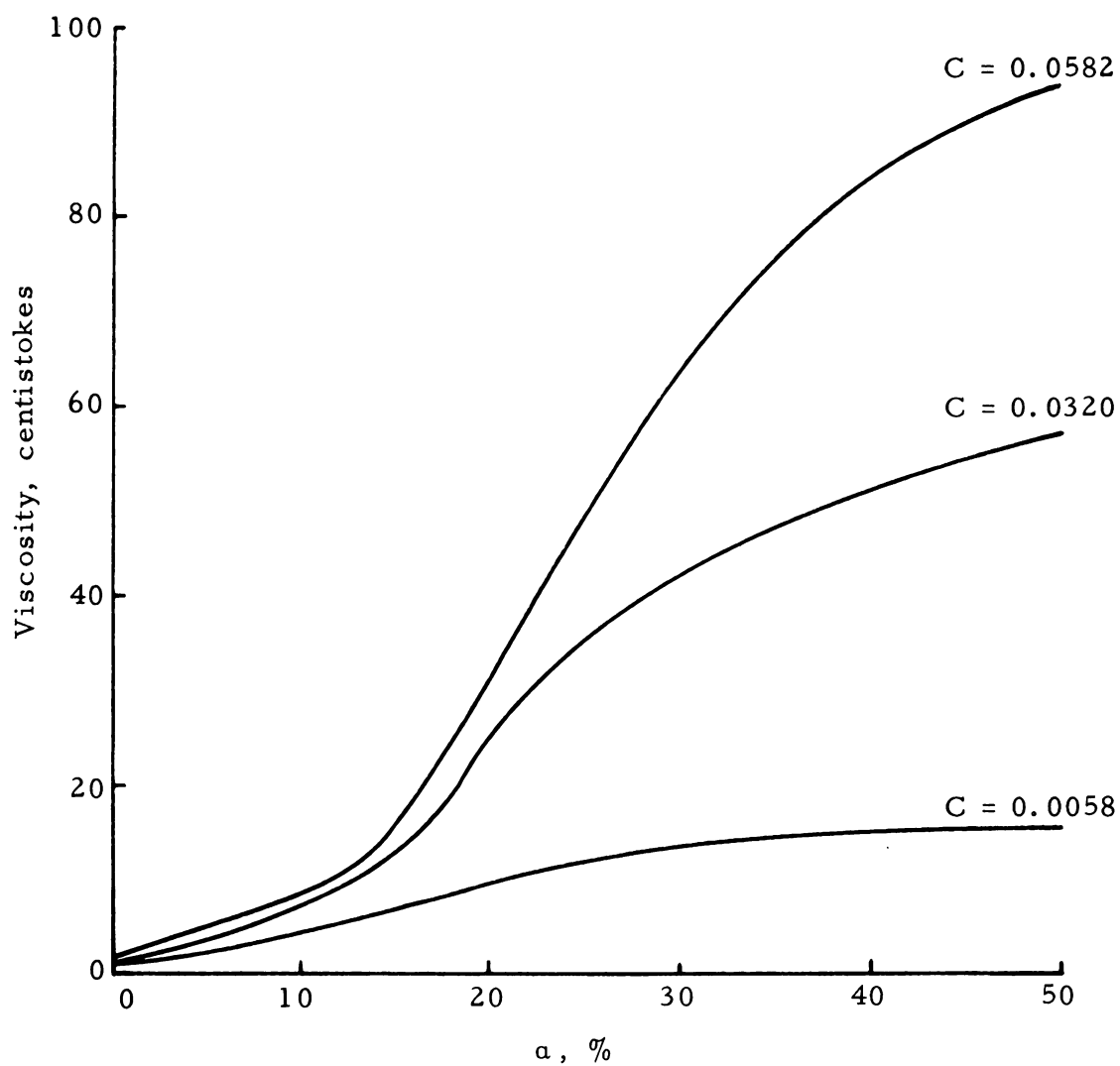
Figure 33. Plot of Apparent Viscosity versus Degree of
Neutralization for PMA Solutions. Molecular
Weight = 470,000.
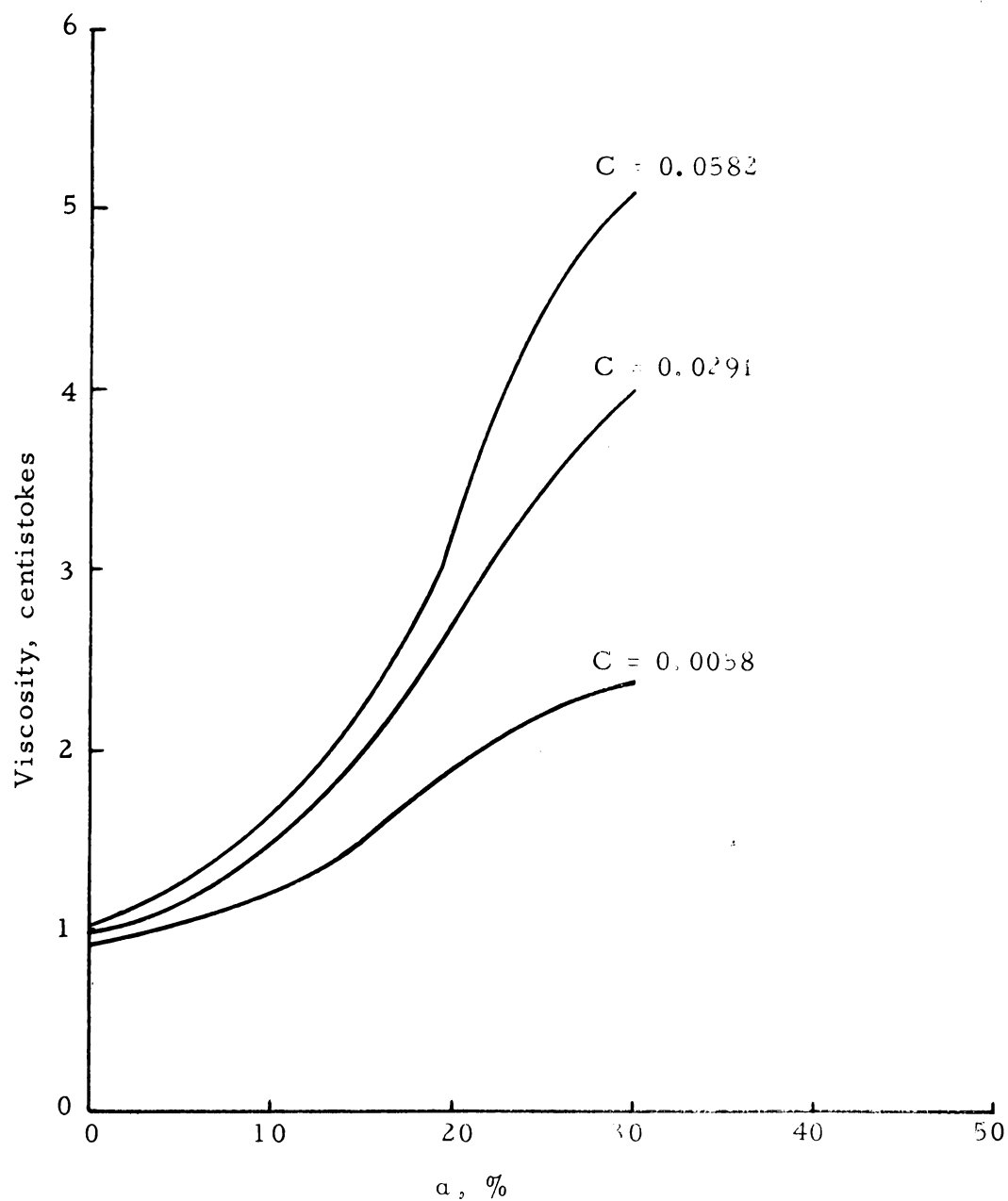
Figure 34. Plot of Apparent Viscosity versus Degree of Neutralization for PMA Solutions. Molecular Weight = 127,000.

The size of the polyion was determined by the procedure out-
lined on page 45. The results are tabulated in Table I for different
degrees of ionization and different concentrations. These values
for the size of the polyion can be compared to the fully extended length
of 6.500 $\overset{o}{A}$. The fully extended length of the polyion is the maximum
extension of the chain, which is calculated from the bond angles and
bond distances between the carbon atoms in the polyion chain. It is
observed that at low concentration and high degree of neutralization
the measured length of the polyion approaches the fully extended length
of the polyion. This suggests that the chain is nearly completely
extended at low concentration and high degree of neutralization.

Table I

Polyion Size of Polymethacrylic Acid and Rotational
Diffusion Constants of Polymethacrylic Acid Solutions

a, %	Concentration (monomoles/liter)	$D_r(sec^{-1})$	Length (Å)
50	0.0058	38.3	6,000
50	0.0116	76.5	5,180
50	0.0213	191	3,830
50	0.0291	383	3,040
10	0.0058	3800	1,410

Fully extended length = 6,500 Å

CONCLUSIONS

The diffusion coefficient of polyelectrolytes has been shown to depend greatly upon the size and shape of the polyion and the degree of ionization. The dependence upon the size and shape is attributed to the change in the hydrodynamic resistance of the polyion and the dependence upon the degree of ionization is the result of the Nernst potential of the counterions. The Nernst potential, as explained earlier, is due to the difference in mobility between the counterions and the polyion. The counterions have a greater mobility and therefore actually drag the polyions with them in the diffusion process. The effect of the Nernst potential was illustrated by the suppression of the ionization of the cations by the addition of sodium thiocyanate. This addition of an electrolyte decreased the diffusion coefficient of potassium polyphosphate by a factor of 60.

In the diffusion of polymethacrylic acid it was observed that the polyion rapidly increased in size as the degree of neutralization was increased. The increase in size of the polyion caused a decrease in the diffusion coefficient because of the increase in the hydrodynamic resistance of the polyion. In the case of low concentration, two depressions in the diffusion coefficient were observed, which indicates a two step opening of the coiled polyion chain. The two step process might be due to a different ionization constant of the acid groups on the inside of the polyion from that of the acid groups on the outside of the polyion. Originally it was assumed that the ionization constant was the same for all the acid groups.

74

Another possible explanation for the data presented, is that the first abrupt change in the size of the polyion is due to the breaking of hydrogen bonds, resulting in an expansion of the coiled polyion; and the second abrupt increase in size is due to an uncoiling of the polyion, in which the polyion approaches a rod-like structure.

The size and shape of the polyion was determined by measuring the electrical anisotropy effect of aqueous polymethacrylic acid solutions. The results of these measurements verified that the depression in the diffusion coefficient was due to the increase in size of the polyion. It was also noted that the measured length of the polyion at high degrees of neutralization and low concentration approaches the fully extended length of the polyion for polymethacrylic acid. Therefore the polyion is nearly completely extended at low concentration and high degree of neutralization.

BIBLIOGRAPHY

1. Anderson, D. K., $\underline{Ph. D.}$ Thesis, University of Washington (1960).

2. Bidlack, D. L., $\underline{Ph. D.}$ Thesis, Michigan State University (1964).

3. Billmeyer, F. W., $\underline{Textbook\ of\ Polymer\ Chemistry}$, Interscience Publishers, Inc., N. Y., 1957, pp. 128-138.

4. Caldwell, C. S., $\underline{Ph. D.}$ Thesis, University of Washington (1955).

5. Caldwell, C. S., Hall, J. R., and Babb, A. L., Rev. Sci. Instr., $\underline{28}$, 816 (1957).

6. Callis, C. F., Van Wasser, J. R., Arvan, P. G., Chem. Revs., $\underline{54}$, 777 (1954).

7. Coulson, C., Cox, J., Ogston, A., and Philpot, J., Proc. Roy. Soc. (London), $\underline{A192}$, 382 (1948).

8. Cohn, J. E. and Edsall, J. T., $\underline{Proteins,\ Anino\ Acids\ and\ Peptids}$ $\underline{as\ Ions\ and\ Dipolar\ Ions}$, Reinhold, N. Y., 1943, p. 624.

9. Eigen, M. and Schwarz, G., J. Colloid Sci., $\underline{12}$, 181 (1957).

10. Fenske, M. and Cannon, M., Ind. Eng. Chem., Anal. Ed., $\underline{10}$, 297 (1938).

11. Fick, A., Ann. Phys. Chem., $\underline{94}$, 59 (1855).

12. Flory, P. J., J. Am. Chem. Soc., $\underline{65}$, 375 (1943).

13. Gans, R., Ann. Physik (4F) $\underline{86}$, 628 (1928).

14. Gotz, K. G., J. Colloid Sci., $\underline{20}$, 289 (1965).

15. Gotz, K. and Heckman, K., J. Colloid Sci., $\underline{13}$, 266 (1958).

16. Harris, F. E., and Rice, S. A., J. Polymer Sci., $\underline{15}$, 151 (1955).

17. Heckman, K., Z. Phys. Chem., $\underline{9}$, 318 (1956).

18. Heckman, K., and Gotz, K., Z. Electrochem., 62, 281, (1958).

19. Huizenga, J. R., Grieger, P. F., and Wall, F. T., J. Am. Chem. Soc., 72, 4228 (1950).

20. Jaenicke, R., Z. Physik. Chem. (Frankfurt) (N.F.), 19, 315 (1959).

21. Jacobson, B., Rev. Sci. Instr., 24, 949 (1953).

22. Jeffery, G. B., Proc. Roy. Soc. (London), A102, 171 (1923).

23. Jerrard, H. G., J. Appl. Phys., 21, 1007 (1950).

24. Katchalsky, A., J. Polymer Sci., 7, 393 (1950).

25. Katchalsky, A., and Eisenberg, H., J. Polymer Sci., 6, 145 (1951).

26. Katchalsky, A., and Lifson, S., J. Polymer Sci., 11, 409 (1953).

27. Katchalsky, A., and Lifson, S., J. Polymer Sci., 13, 52 (1954).

28. Katchman, B. J., and Smith, H. E., Archives of Biochemistry and Biophysics, 75, 396 (1958).

29. Kedem, O., and Katchalsky, A., J. Polymer Sci., 15, 321 (1955).

30. Kern, W., Z. Physik. Chem., A181, 249 (1938).

31. Kuhn, W., Z. Physik. Chem. (Leipzig), A161, 1 (1932).

32. Kuhn, W., and Kuhn, H., Helv. Chim. Acta., 26, 1394 (1936).

33. Longsworth, L. G., Rev. Sci. Instr., 21, 524 (1950).

34. Mach, L., Sitz. Wiener Akad., 101, IIA, 5 (1892).

35. Malmgren, H., Actachemica Scandinanica, 2, 147 (1948).

36. Nernst, W., Z. Physik. Chem., 2, 613 (1888).

37. Nagasaw, M. and Fujita, H., J. Am. Chem. Soc., 86, 3005 (1964).

38. Oth, A. and Doty, P., J. Phys. Chem., 56, 43 (1952).

39. Peterlin, A., Z. Physik, 111, 232 (1938).

40. Perrin, F., J. Phys. Radium (7), 5, 497 (1934).

41. Rice, S. A. and Nagasawa, M., Polyelectrolyte Solutions, Academic Press, N. Y., 1961.

42. Schwarz, G., Z. Physik, 145, 563 (1956).

43. Taylor, G. J., Proc. Roy. Soc. (London), A157, 546 (1936).

44. Van Wasser, J. R., and Holst, K. A., J. Am. Chem. Soc., 72, 639 (1950).

45. Van Wasser, J. R., J. Am. Chem. Soc., 72, 906 (1950).

46. Van Wasser, J. R., Griffith, E. J., and McCullough, J. F., J. Am. Chem. Soc., 74, 4978 (1952).

47. Vink, H., Makro. Chem., 67, 105 (1963).

48. Vithani, K. K., M. S. Thesis, Michigan State University (1960).

49. Voet, A., J. Phys. Chem., 51, 1037 (1947).

50. Wiener, O., Wied. Ann., 49, 105 (1893).

51. Zehnder, L., Z. Instrumentenk., 11, 275 (1891).

APPENDICES

Appendix I

Sample Calculation of Diffusion Coefficient

Experimental run number: A-6

Date: July 29, 1963

Diffusion of potassium polyphosphate in aqueous solution.

Solution A (For upper level of diffusion cell)

$$C_1 = 6 \text{ gm } (KPO_3)_n / \text{liter}$$

Solution B (For lower level of diffusion cell)

$$C_2 = 3 \text{ gm } (KPO_3)_n / \text{liter}$$

See Figure 9 for actual photographic plate.

Exposure number	Time, minutes
1	0
2	5
3	10
4	15
5	20
6	25
7	30
8	40
9	45
10	51
11	55
12	60
13	65
14	70

$J = 15$

Exposure 2,   t = 5 minutes

(For definition of measurements see Figure 13)

j	$(x'_o - x'_j)$, cm.	k	$(x'_o + x'_k)$, cm.	$[(x'_o + x'_k) - (x'_o - x'_j)]$, cm.
2	2.703	8	2.921	0.218
3	2.756	9	2.951	0.195
4	2.797	10	2.982	0.185
5	2.833	11	3.014	0.181
6	2.863	12	3,054	0.191
7	2.893	13	3.103	0.210

Exposure 4,   t = 15 minutes

j	$(x'_o - x'_j)$, cm.	k	$(x'_o + x'_k)$, cm.	$[(x'_o + x'_k) - (x'_o - x'_j)]$, cm.
2	2.616	8	2.923	0.307
3	2.692	9	2.965	0.273
4	2.747	10	3.008	0.261
5	2.795	11	3.055	0.260
6	2.841	12	3.108	0.267
7	2.883	13	3.180	0.297

Exposure 7,   t = 30 minutes

j	$(x'_o - x'_j)$, cm.	k	$(x'_o + x'_k)$, cm.	$[(x'_o + x'_k) - (x'_o - x'_j)]$, cm.
2	2.539	8	2.930	0.391
3	2.631	9	2.987	0.356
4	2.702	10	3.039	0.337
5	2.763	11	3.101	0.338
6	2.822	12	3.177	0.355
7	2.879	13	3.266	0.387

Exposure 10, t = 51 minutes

j	$(x'_o - x'_j)$, cm.	k	$(x'_o + x'_k)$, cm.	$[(x'_o + x'_k) - (x'_o - x'_j)]$, cm.
2	2.408	8	2.892	0.484
3	2.517	9	2.957	0.440
4	2.606	10	3.024	0.418
5	2.687	11	3.101	0.414
6	2.757	12	3.192	0.435
7	2.827	13	3.304	0.477

Exposure 12, t = 60 minutes

j	$(x'_o - x'_j)$, cm.	k	$(x'_o + x'_k)$, cm.	$[(x'_o + x'_k) - (x'_o - x'_j)]$, cm.
2	2.355	8	2.880	0.525
3	2.477	9	2.950	0.473
4	2.575	10	3.025	0.450
5	2.656	11	3.107	0.451
6	2.735	12	3.197	0.462
7	2.812	13	3.315	0.503

Exposure 14, t = 70 minutes

j	$(x'_o - x'_j)$, cm.	k	$(x'_o + x'_k)$, cm.	$[(x'_o + x'_k) - (x'_o - x'_j)]$, cm.
2	2.329	8	2.872	0.543
3	2.442	9	2.949	0.507
4	2.548	10	3.028	0.480
5	2.638	11	3.111	0.473
6	2.718	12	3.208	0.490
7	2.801	13	3.335	0.534

j	$J - 2j$	$\dfrac{J - 2j}{J}$	$\mathrm{erf}^{-1}\left(\dfrac{J-2j}{J}\right) \equiv A$
2	11	0.7333	0.7850
3	9	0.6000	0.5950
4	7	0.4667	0.4405
5	5	0.3333	0.3046
6	3	0.2000	0.1792
7	1	0.0667	0.0592

k	$2k - J$	$\dfrac{2k - J}{J}$	$\mathrm{erf}^{-1}\left(\dfrac{2k-J}{J}\right) \equiv B$
8	1	0.0667	0.0592
9	3	0.2000	0.1792
10	5	0.3333	0.3046
11	7	0.4667	0.4405
12	9	0.6000	0.5950
13	11	0.7333	0.7850

$A + B$	$\dfrac{1}{A + B}$
0.8442	1.1846
0.7742	1.2916
0.7451	1.3421
0.7451	1.3421
0.7742	1.2916
0.8442	1.1846

Exposure 2

$(x_k' + x_j')$, cm.	$\left(\dfrac{x_k' + x_j'}{A+B}\right)$, cm.
0.218	0.2582
0.195	0.2519
0.185	0.2483
0.181	0.2429
0.191	0.2467
0.210	0.2488
average	0.2495

$$\left(\frac{x_k' + x_j'}{A+B}\right)^2_{avg.} = 0.06225 \text{ cm}^2$$

Exposure 4

$(x'_k + x'_j)$, cm.	$\left(\dfrac{x'_k + x'_j}{A+B}\right)$, cm.
0.307	0.363.7
0.273	0.352.6
0.261	0.350.3
0.260	0.348.9
0.267	0.344.9
0.297	0.351.8
average	0.352.0

$$\left(\frac{x'_k + x'_j}{A+B}\right)^2_{avg.} = 0.1239 \ cm^2$$

Exposure 7

$(x'_k + x'_j)$, cm.	$\left(\dfrac{x'_k + x'_j}{A+B}\right)$, cm.
0.391	0.4632
0.356	0.4598
0.337	0.4523
0.338	0.4536
0.355	0.4585
0.387	0.4584
average	0.4526

$$\left(\frac{x'_k + x'_j}{A+B}\right)^2_{avg.} = 0.2094 \ cm^2$$

Exposure 10

$(x'_k + x'_j)$, cm.	$\left(\dfrac{x'_k + x'_j}{A+B}\right)$, cm.
0.484	0.5733
0.440	0.5683
0.418	0.5610
0.414	0.5556
0.435	0.5618
0.477	0.5651
average	0.5642

$$\left(\frac{x'_k + x'_j}{A+B}\right)^2_{avg.} = 0.3183 \ cm^2$$

Exposure 12

$(x'_k + x'_j)$, cm.	$\left(\dfrac{x'_k + x'_j}{A+B}\right)$, cm.
0.525	0.6195
0.473	0.6109
0.450	0.6039
0.451	0.6053
0.462	0.5967
0.503	0.5959
average	0.6054

$$\left(\frac{x'_k + x'_j}{A+B}\right)^2_{avg.} = 0.3665 \text{ cm}^2$$

Exposure 14

$(x'_j + x'_k)$, cm.	$\left(\dfrac{x'_k + x'_j}{A+B}\right)$, cm.
0.543	0.6432
0.507	0.6548
0.480	0.6442
0.473	0.6348
0.490	0.6329
0.534	0.6326
average	0.6404

$$\left(\frac{x'_k + x'_j}{A+B}\right)^2_{avg.} = 0.4101 \text{ cm}^2$$

Slope of the plot of $\left(\dfrac{x'_k + x'_j}{A+B}\right)^2_{avg.}$ versus time, t is

0.922×10^{-4} cm.^{2}/sec. See Figure 35.

$$D = \frac{\text{slope}}{4M^2} = \frac{0.922 \times 10^{-4}}{14.792} = 6.23 \times 10^{-6} \text{ cm.}^2/\text{sec.}$$
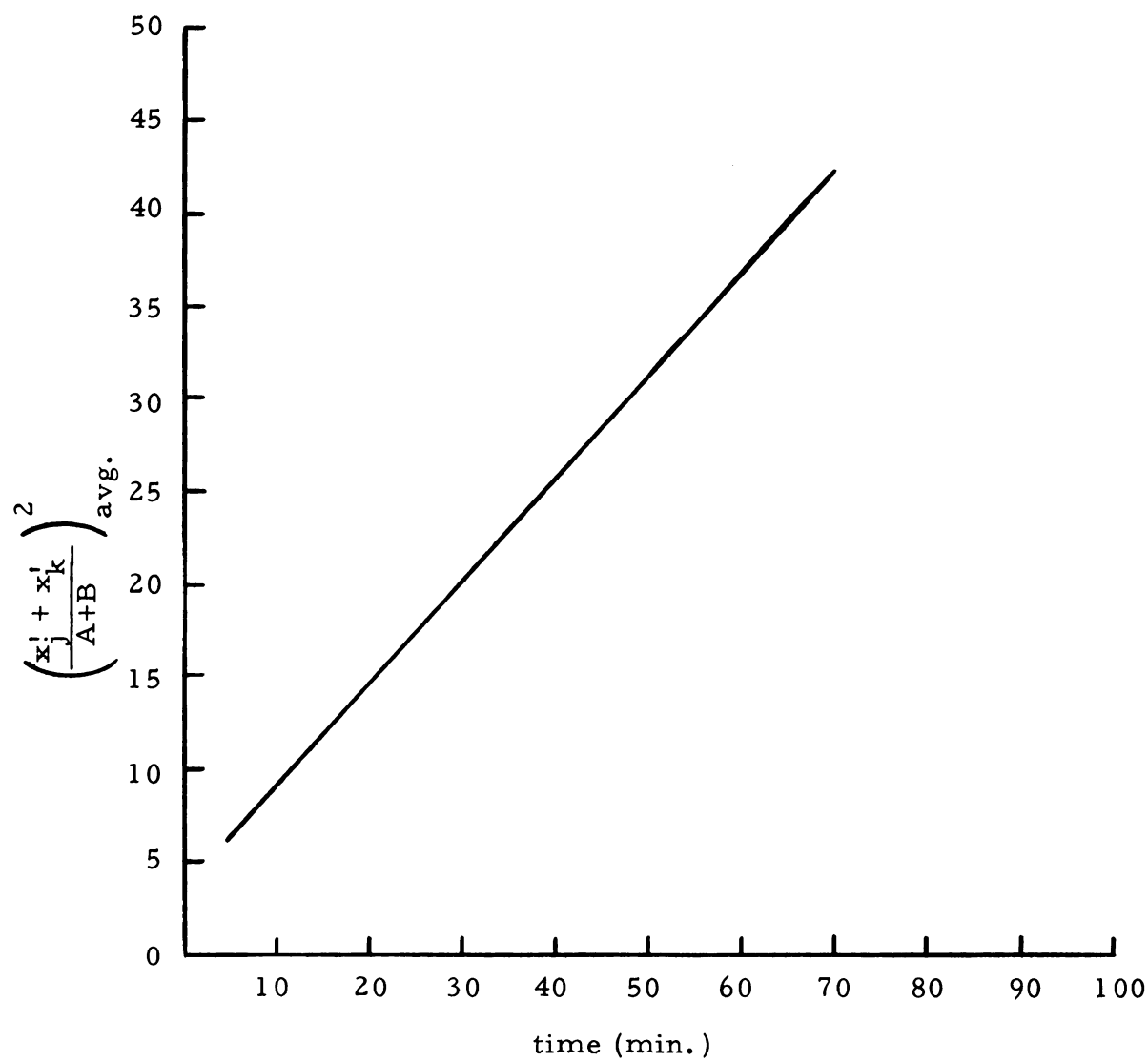
Figure 35. Plot of $\left(\dfrac{x'_j + x'_k}{A+B}\right)^2$ versus Time.

Table II

Diffusion Data for Potassium Polyphosphate Solutions

Run No.	Concentration (In lower half of cell) g/l	Concentration (In upper half of cell) g/l	$D \times 10^6$ cm^2/sec
A-2	5	0	6.28
A-3	5	0	6.60
A-4	5 (In 0.4 M NaSCN)	0.4 M NaSCN	0.10
A-5	5	1	4.90
A-6	6	3	6.23

Table III

Diffusion Data for Polymethacrylic Acid Solutions at an Average
Concentration = 0.0320 Monomoles/liter, Molecular Weight
= 127,000.

Run No.	a, %	$D \times 10^6$ (cm^2/sec)
C-1	0	1.772
C-2	5	2.430
C-3	10	4.185
C-4	15	3.663
C-5	20	4.617
C-6	30	4.816
B-2	50	5.039

Table IV

Diffusion Data for Polymethacrylic Acid Solutions at an Average

Concentration = 0.0213 Monomoles/liter, Molecular Weight = 357,000.

Run No.	α, %	$D \times 10^6$ (cm^2/sec)
D-1	0	2.384
D-2	5	4.190
D-3	10	4.931
D-12	11.25	4.725
D-8	12.5	4.553
D-4	15	4.904
D-13	17.5	5.000
D-5	20	5.032
D-11	22.5	4.683
D-6	25	4.896
D-10	30	5.055
D-7	40	5.284
D-14	50	5.498

Table V

Diffusion Data for Polymethacrylic Acid Solutions at an Average

Concentration = 0.0213 Monomoles/liter, Molecular Weight = 860,000.

Run No.	a, %	$D \times 10^6$ (cm^2/sec)
E-11	0	2.668
E-2	5	4.081
E-3	10	4.926
E-14	12.5	4.569
E-5	15	4.912
E-6	17.5	5.087
E-7	20	4.676
E-8	22.5	4.875
E-9	25	5.193
E-10	30	5.408
E-12	40	5.530
E-13	50	5.762

Table VI

Diffusion Data for Polymethacrylic Acid Solutions at an Average

Concentration = 0.0320 Monomoles/liter, Molecular Weight = 470,000.

Run No.	α, %	$D \times 10^6$ (cm^2/sec)
F-1	0	1.810
F-2	5	3.906
F-3	10	4.754
F-4	12.5	4.562
F-5	15	4.432
F-6	17.5	4.733
F-7	20	4.993
F-8	25	4.167
F-9	30	5.162
F-10	40	5.278
F-11	50	5.516

Table VII

Apparent Viscosities of Polymethacrylic Acid Solutions
Molecular Weight = 127,000

a, %	η (centistokes) C = 0.0582 (monomoles/liter)	η (centistokes) C = 0.0291 (monomoles/liter)	η (centistokes) C = 0.0058 (monomoles/liter)
0	1.037	0.984	0.939
5	1.236	1.123	1.035
10	1.730	1.530	1.177
15	2.260	1.976	1.499
20	3.207	2.708	1.880
30	5.102	4.007	2.383

Table VIII

Apparent Viscosities of Polymethacrylic Acid Solutions
Molecular Weight = 357,000

a, %	η (centistokes C = 0.0388 (monomoles/liter)	η (centistokes) C = 0.0213 (monomoles/liter)	η (centistokes) C = 0.0039 (monomoles/liter)
0	1.406	1.286	1.176
5	3.204	--	1.899
10	4.946	3.880	2.465
15	7.994	6.430	3.693
17.5	9.247	7.349	4.099
20	11.744	9.159	4.635
22.5	12.854	10.080	5.058
25	14.965	10.738	5.562
30	19.169	13.338	5.790
40	22.377	15.535	6.199
50	23.296	16.147	6.214

Table IX

Apparent Viscosities of Polymethacrylic Acid Solutions
Molecular Weight = 860,000

a,%	η (centistokes) C = 0.0388 (monomoles/liter)	η (centistokes) C = 0.0213 (monomoles/liter)	η (centistokes) C = 0.0039 (monomoles/liter)
0	3.800	3.408	1.561
5	8.263	6.845	4.171
10	13.216	11.631	5.264
12.5	16.452	14.890	7.205
15	28.874	23.052	7.844
17.5	39.690	29.865	9.591
20	51.278	34.962	10.092
22.5	62.924	41.352	10.776
25	77.707	48.313	11.184
30	115.717	65.598	12.576
40	155.160	80.237	13.012
50	176.297	86.405	14.197

Table X

Apparent Viscosities of Polymethacrylic Acid Solutions
Molecular Weight = 470,000

a, %	η (centistokes) C = 0.0582 (monomoles/liter)	η (centistokes) C = 0.0320 (monomoles/liter)	η (centistokes) C = 0.0058 (monomoles/liter)
0	1.871	1.608	1.322
5	4.986	4.233	2.660
10	8.005	7.175	4.061
12.5	10.751	9.438	5.371
15	15.757	13.093	6.374
17.5	23.244	18.384	8.193
20	37.278	26.029	10.119
25	48.489	34.310	12.030
30	62.555	41.779	12.855
40	84.146	51.147	14.748
50	93.783	57.361	15.787

Table X

Apparent Viscosities of Polymethacrylic Acid Solutions
Molecular Weight = 470, 000

a, %	η (centistokes) C = 0.0582 (monomoles/liter)	η (centistokes) C = 0.0320 (monomoles/liter)	η (centistokes) C = 0.0058 (monomoles/liter)
0	1.871	1.608	1.322
5	4.986	4.233	2.660
10	8.005	7.175	4.061
12.5	10.751	9.438	5.371
15	15.757	13.093	6.374
17.5	23.244	18.384	8.193
20	37.278	26.029	10.119
25	48.489	34.310	12.030
30	62.555	41.779	12.855
40	84.146	51.147	14.748
50	93.783	57.361	15.787

Appendix III

Table XI

Conductivity Data from Couette Apparatus
Concentration = 0.0291 monomoles P.M.A./liter

0% Neutralization

RPM	$K \times 10^5$ mhos	$(K - K_o)/K_o \times 10^2$
0	1.134	0
100	1.135	0.088
200	1.135	0.088
300	1.135	0.088
400	1.132	-0.176
500	1.135	0.088
600	1.135	0.088
700	1.136	0.176
800	1.135	0.088

5% Neutralization

RPM	$K \times 10^5$ mhos	$(K - K_o)/K_o \times 10^2$
0	1.028	0
100	1.029	0.097
200	1.030	0.194
300	1.030	0.194
400	1.030	0.194
500	1.031	0.292
600	1.032	0.389
700	1.033	0.486
800	1.035	0.681

94

10% Neutralization

RPM	$K \times 10^5$ mhos	$(K - K_o)/K_o \times 10^2$
0	1.724	0
100	1.727	0.174
200	1.730	0.348
300	1.733	0.522
400	1.733	0.522
500	1.730	0.348
600	1.736	0.696
700	1.742	1.044
800	1.742	1.044

15% Neutralization

RPM	$K \times 10^5$ mhos	$(K - K_o)/K_o \times 10^2$
0	2.439	0
100	2.451	0.741
200	2.463	0.984
300	2.469	1.230
400	2.475	1.476
500	2.481	1.722
600	2.488	2.009
700	2.488	2.009
800	2.494	2.255

20% Neutralization

RPM	$K \times 10^5$ mhos	$(K - K_o)/K_o \times 10^2$
0	3.164	0
100	3.185	0.664
200	3.195	0.980
300	3.215	1.612
400	3.226	1.960
500	3.236	2.276
600	3.247	2.623
700	3.257	2.939
800	3.268	3.287

25% Neutralization

RPM	$K \times 10^5$ mhos	$(K - K_o)/K_o \times 10^2$
0	3.846	0
100	3.876	0.780
200	3.906	1.560
300	3.922	1.976
400	3.937	2.366
500	3.937	2.366
600	3.937	2.366
700	3.937	2.366
800	3.937	2.366
900	3.952	2.756

30% Neutralization

RPM	$K \times 10^5$ mhos	$(K - K_o)/K_o \times 10^2$
0	4.484	0
100	4.525	0.914
200	4.566	1.829
300	4.587	2.297
400	4.608	2.765
500	4.608	2.765
600	4.608	2.765
700	4.630	3.256
800	4.651	3.724

40% Neutralization

RPM	$K \times 10^5$ mhos	$(K - K_o)/K_o \times 10^2$
0	4.854	0
100	4.901	0.968
200	4.950	1.978
300	5.000	3.008
400	5.025	3.523
500	5.050	4.038
600	5.076	4.574
700	5.102	5.109
800	5.128	5.645
900	5.155	6.201
1000	5.155	6.201

50% Neutralization

RPM	$K \times 10^5$ mhos	$(K - K_o)/K_o \times 10^2$
0	6.452	0
100	6.562	1.565
200	6.614	2.511
300	6.667	3.332
400	6.711	4.014
500	6.748	4.588
600	6.780	5.084
700	6.807	5.502
800	6.831	5.874
900	6.863	6.370
1000	6.887	6.742

Table XII

Conductivity Data from Couette Apparatus
Concentration = 0.0116 monomoles P.M.A./liter

0% Neutralization

RPM	$K \times 10^6$ mhos	$(K - K_o)/K_o$
0	5.84	0
100	5.84	0
200	5.84	0
300	5.84	0
400	5.84	0
500	5.84	0
600	5.84	0
700	5.84	0
800	5.84	0
900	5.84	0
100	5.84	0

5% Neutralization

RPM	$K \times 10^6$ mhos	$(K - K_o)/K_o$
0	6.11	0
100	6.13	0.0032
200	6.14	0.0049
300	6.15	0.0065
400	6.16	0.0081
500	6.17	0.0098
600	6.18	0.0114
700	6.19	0.0131
800	6.20	0.0147
900	6.21	0.0164
1000	6.22	0.0180

10% Neutralization

RPM	$K \times 10^6$ mhos	$(K - K_o)/K_o$
0	12.30	0
100	12.40	0.0081
200	12.50	0.0163
300	12.55	0.0203
400	12.60	0.0244
500	12.65	0.0285
600	12.70	0.0325
700	12.75	0.0366
800	12.80	0.0406
900	12.83	0.0431
1000	12.85	0.0447

15% Neutralization

RPM	$K \times 10^5$ mhos	$(K - K_o)/K_o$
0	1.727	0
100	1.770	0.0249
200	1.776	0.0284
300	1.786	0.0342
400	1.795	0.0393
500	1.805	0.0452
600	1.812	0.0492
700	1.818	0.0527
800	1.825	0.0567
900	1.832	0.0608
1000	1.838	0.0643

20% Neutralization

RPM	$K \times 10^5$ mhos	$(K - K_o)/K_o$
0	1.282	0
100	1.302	0.0156
200	1.312	0.0234
300	1.326	0.0328
400	1.335	0.0413
500	1.342	0.0468
600	1.351	0.0538
700	1.355	0.0569
800	1.360	0.0608
900	1.366	0.0655
1000	1.370	0.0686

25% Neutralization

RPM	$K \times 10^5$ mhos	$(K - K_o)/K_o$
0	1.565	0
100	1.600	0.0224
200	1.618	0.0339
300	1.634	0.0441
400	1.645	0.0511
500	1.650	0.0543
600	1.656	0.0581
700	1.661	0.0613
800	1.667	0.0652
900	1.672	0.0684
1000	1.675	0.0703

30% Neutralization

RPM	$K \times 10^5$ mhos	$(K - K_o)/K_o$
0	1.798	0
100	1.862	0.0356
200	1.880	0.0456
300	1.898	0.0556
400	1.912	0.0634
500	1.927	0.0717
600	1.934	0.0756
700	1.941	0.0795
800	1.949	0,0840
900	1.957	0.0884
1000	1.965	0.0929

40% Neutralization

RPM	$K \times 10^5$ mhos	$(K - K_o)/K_o$
0	3.279	0
100	3.401	0.0372
200	3.448	0.0515
300	3.497	0.0665
400	3.534	0.0777
500	3.571	0.0890
600	3.597	0.0970
700	3.623	0.1049
800	3.650	0.1131
900	3.663	0.1171
1000	3.690	0.1253

50% Neutralization

RPM	$K \times 10^5$ mhos	$(K - K_o)/K_o$
0	2.577	0
100	2.667	0.0349
200	2.725	0.0574
300	2.770	0.0749
400	2.809	0.0900
500	2.841	0.1204
600	2.865	0.1118
700	2.890	0.1214
800	2.907	0.1280
900	2.924	0.1346
1000	2.941	0.1412

Table XIII

Conductivity Data from Couette Apparatus
Concentration = 0.0213 monomoles P.M.A./liter

0% Neutralization

RPM	$K \times 10^6$ mhos	$(K - K_o)/K_o \times 10^2$
0	8.60	0
100	8.60	0
200	8.60	0
300	8.60	0
400	8.60	0
500	8.60	0
600	8.60	0
700	8.60	0
800	8.60	0
900	8.60	0
1000	8.60	0

5% Neutralization

RPM	$K \times 10^5$ mhos	$(K - K_o)/K_o \times 10^2$
0	1.063	0
100	1.064	0.094
200	1.065	0.188
300	1.066	0.282
400	1.066	0.282
500	1.067	0.376
600	1.068	0.470
700	1.068	0.470
800	1.070	0.658
900	1.071	0.753
1000	1.071	0.753

10% Neutralization

RPM	$K \times 10^5$ mhos	$(K - K_o)/K_o \times 10^2$
0	1.887	0
100	1.887	0
200	1.894	0.371
300	1.898	0.583
400	1.901	0.742
500	1.905	0.954
600	1.908	1.113
700	1.912	1.325
800	1.916	1.537
900	1.916	1.537
1000	1.919	1.696

15% Neutralization

RPM	$K \times 10^5$ mhos	$(K - K_o)/K_o \times 10^2$
0	1.760	0
100	1.770	0.568
200	1.779	1.080
300	1.786	1.477
400	1.792	1.818
500	1.798	2.159
600	1.805	2.557
700	1.812	2.955
800	1.815	3.125
900	1.821	3.466
1000	1.825	3.693

20% Neutralization

RPM	$K \times 10^5$ mhos	$(K - K_o)/K_o \times 10^2$
0	2.481	0
100	2.506	1.008
200	2.525	1.773
300	2.538	2.297
400	2.544	2.539
500	2.551	2.821
600	2.564	3.345
700	2.571	3.628
800	2.577	3.869
900	2.584	4.152
1000	2.591	4.434

25% Neutralization

RPM	$K \times 10^5$ mhos	$(K - K_o)/K_o \times 10^2$
0	2.817	0
100	2.849	1.136
200	2.865	1.704
300	2.882	2.307
400	2.898	2.875
500	2.907	3.195
600	2.924	3.798
700	2.932	4.082
800	2.941	4.402
900	2.950	4.721
1000	2.958	5.005

30% Neutralization

RPM	$K \times 10^5$ mhos	$(K - K_o)/K_o \times 10^2$
0	3.401	0
100	3.448	1.382
200	3.472	2.088
300	3.496	2.793
400	3.509	3.176
500	3.521	3.528
600	3.534	3.911
700	3.546	4.263
800	3.559	4.646
900	3.565	4.822
1000	3.571	4.998

40% Neutralization

RPM	$K \times 10^5$ mhos	$(K - K_o)/K_o \times 10^2$
0	4.115	0
100	4.184	1.677
200	4.219	2.527
300	4.255	3.402
400	4.292	4.301
500	4.310	4.739
600	4.329	5.200
700	4.348	5.662
800	4.367	6.124
900	4.386	6.586
1000	4.405	7.047

50% Neutralization

RPM	$K \times 10^5$ mhos	$(K - K_o)/K_o \times 10^2$
0	4.237	0
100	4.329	2.171
200	4.367	3.068
300	4.405	3.965
400	4.444	4.886
500	4.484	5.830
600	4.525	6.797
700	4.556	7.529
800	4.587	8.260
900	4.620	9.039
1000	4.651	9.771

Table XIV

Conductivity Data from Couette Apparatus

Concentration = 0.0058 monomoles P.M.S./liter

0% Neutralization

RPM	$K \times 10^6$ mhos	$(K - K_o)/K_o \times 10^3$
0	3.16	0
100	3.17	3.153
200	3.16	0
300	3.17	3.153
400	3.16	0
500	3.17	3.153
600	3.17	3.153
700	3.17	3.153
800	3.17	3.153

5% Neutralization

RPM	$K \times 10^6$ mhos	$(K - K_o)/K_o \times 10^2$
0	3.48	0
100	3.50	0.575
200	3.51	0.862
300	3.52	1.149
400	3.53	1.437
500	3.54	1.724
600	3.55	2.011
700	3.57	2.586
800	3.58	2.874

10% Neutralization

RPM	$K \times 10^6$ mhos	$(K - K_o)/K_o \times 10^2$
0	5.71	0
100	5.83	2.102
200	5.89	3.152
300	5.93	3.853
400	5.97	4.553
500	6.01	5.254
600	6.05	5.954
700	6.09	6.655
800	6.11	7.005
900	6.13	7.356
1000	6.13	7.356

15% Neutralization

RPM	$K \times 10^6$ mhos	$(K - K_o)/K_o \times 10^2$
0	86.3	0
100	88.7	2.781
200	90.0	4.287
300	91.0	5.446
400	91.8	6.373
500	92.3	6.952
600	92.8	7.532
700	93.3	8.111
800	93.8	8.691
900	94.2	9.154

12.5% Neutralization

RPM	$K \times 10^6$ mhos	$(K - K_o)/K_o$
0	6.35	0
100	6.53	0.0283
200	6.62	0.0472
300	6.69	0.0535
400	6.75	0.0630
500	6.80	0.0709
600	6.85	0.0874
700	6.88	0.0835
800	6.91	0.0882
900	6.95	0.0945
1000	6.98	0.0992

17.5% Neutralization

RPM	$K \times 10^6$ mhos	$(K - K_o)/K_o$
0	8.44	0
100	8.78	0.0403
200	8.90	0.0545
300	8.97	0.0628
400	9.03	0.0699
500	9.05	0.0723
600	9.10	0.0782
700	9.16	0.0853
800	9.21	0.0912
900	9.26	0.0972
1000	9.30	0.1019

20% Neutralization

RPM	$K \times 10^5$ mhos	$(K - K_o)/K_o$
0	1.072	0
100	1.111	0.0364
200	1.136	0.0597
300	1.149	0.0718
400	1.163	0.0849
500	1.168	0.0896
600	1.176	0.0970
700	1.183	0.1035
800	1.190	0.1101
900	1.198	0.1175
1000	1.205	0.1241

25% Neutralization

RPM	$K \times 10^5$ mhos	$(K - K_o)/K_o$
0	1.360	0
100	1.425	0.0478
200	1.447	0.0640
300	1.466	0.0779
400	1.483	0.0904
500	1.497	0.1007
600	1.510	0.1103
700	1.520	0.1176
800	1.529	0.1243
900	1.538	0.1309
1000	1.546	0.1368

30% Neutralization

RPM	$K \times 10^5$ mhos	$(K - K_o)/K_o$
0	1.460	0
100	1.534	0.0507
200	1.562	0.0699
300	1.592	0.0904
400	1.610	0.1027
500	1.629	0.1158
600	1.642	0.1247
700	1.653	0.1322
800	1.667	0.1418
900	1.675	0.1473
1000	1.684	0.1534

40% Neutralization

RPM	$K \times 10^5$ mhos	$(K - K_o)/K_o$
0	1.550	0
100	1.650	0.0645
200	1.681	0.0845
300	1.715	0.1065
400	1.742	0.1239
500	1.760	0.1355
600	1.776	0.1458
700	1.792	0.1561
800	1.805	0.1645
900	1.815	0.1710
1000	1.825	0.1774

50% Neutralization

RPM	$K \times 10^5$ mhos	$(K - K_o)/K_o$
0	1.852	0
100	2.016	0.0885
200	2.075	0.1204
300	2.119	0.1442
400	2.150	0.1609
500	2.183	0.1787
600	2.203	0.1895
700	2.222	0.1998
800	2.237	0.2079
900	2.257	0.2187
1000	2.268	0.2246

Table XV

Relative Change in Conductivity of Polymethacrylic Acid
Solutions in Couette Apparatus at 400 R.P.M., A_{400}

C = 0.0116 Monomoles/Liter

α	A_{400}
0	0
5	0.008
10	0.024
15	0.039
20	0.041
25	0.051
30	0.063
40	0.078
50	0.090

C = 0.0213 monomoles PMA/l

α	$A_{400} \times 10^2$
0	0
5	0.35
10	0.75
15	1.80
20	2.35
25	2.90
30	3.20
40	4.10
50	4.90

C   = 0.0291 monomoles P.M.A./liter

α	A_{400}
0	0.0008
5	0.0025
10	0.0055
15	0.0150
20	0.0195
25	0.0235
30	0.0275
40	0.0350
50	0.0400

C   = 0.0058 monomoles P.M.A./liter

α	A_{400}
0	0.002
5	0.014
10	0.046
15	0.064
20	0.085
25	0.090
30	0.102
40	0.124
50	0.161

Appendix IV

NOMENCLATURE

A   relative change in conductivity

A_{400} relative change in conductivity at 400 R.P.M.

a   one-half the length of rod-shaped particles in Stoke's law, cm.

b   thickness of rod-shaped particles in Stoke's law, cm.

b   shape factor of rotational ellipsoid, equation (26)

b   hydrodynamic length of a monomer, cm., equation (14)

c   concentration, moles/cm.^{3}

c_o concentration at zero position in diffusion cell, moles/cm.^{3}

D   mutual diffusion coefficient, cm.^{2}/sec.

D_e dielectric constant of solvent

D_r rotational diffusion constant, sec.$^{-1}$

DP   degree of polymerization

d   gap width in Couette apparatus, cm.

F   free energy, cal./mole

F_{el} electrostatic free energy, cal./mole

f   fraction of ion binding, equation (5)

f   axial flux, equation (33)

h   average end-to-end distance

h^2 mean square end-to-end distance of polyion

h_o^2 unionized mean square length

J   diffusional flux, moles/cm.^{2}/sec.

J   total number of interference fringes

$\vec{J}_D$ rotational flux of particles due to Brownian movement

117
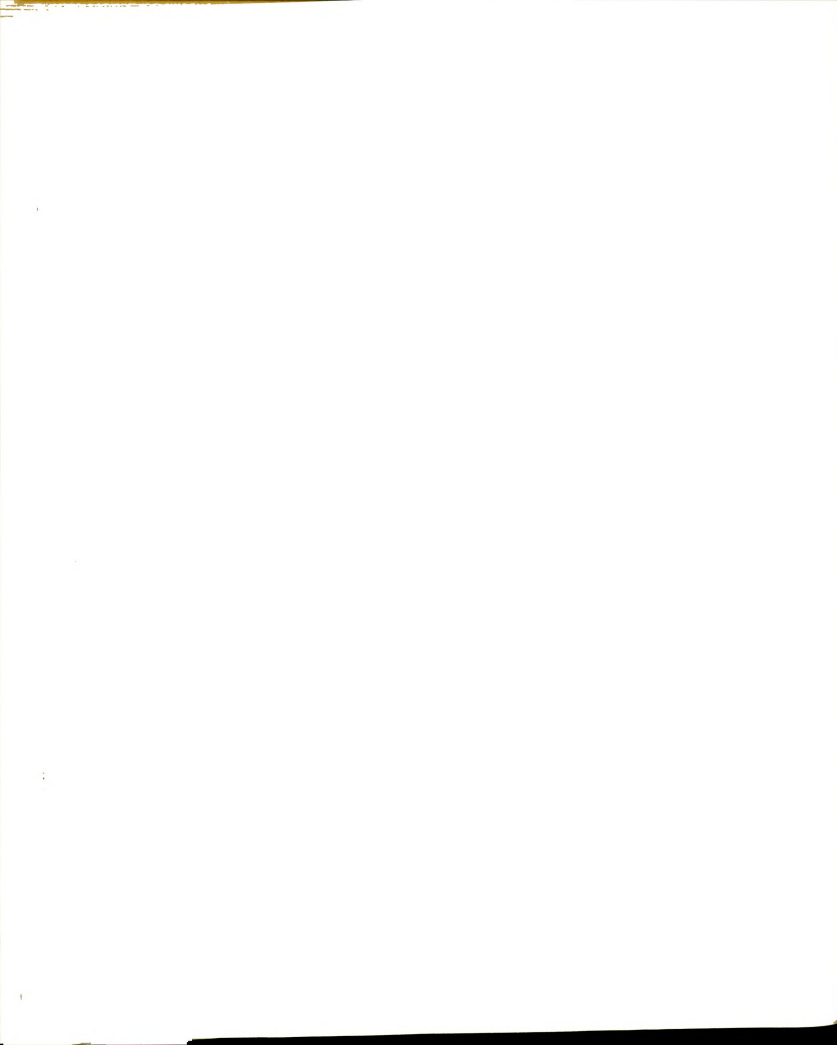
$\vec{J}_F$ rotational flux of particles due to flow

j fringe number in lower level of diffusion cell

K conductivity of solution measured in Couette apparatus

K_o conductivity of solution at rest

$\overline{K}$ conductivity of solution at complete orientation of polyions in Couette apparatus

$K(\sigma)$ normalized anisotropy

k fringe number in upper level of diffusion cell

k Boltzman's constant, 1.380×10^{-16} erg/deg.

l length of polyion, cm. or angstroms

M magnification factor of diffusiometer, 1.923

M_a arbitrary abscissa scale in electrical anisotropy measurements, sec.$^{-1}$/cm.

M_o arbitrary ordinate scale in electrical anisotropy measurements, fraction/cm.

$\overline{M}_v$ average molecular weight

N Avogadro's number, 6.023×10^{23}

N number of particles per unit volume, equation (32)

n refractive index, equation (39)

n moles of solute per milliliter, equation (2)

n_i number of ions of type i per macromolecule

P parameter used in Figure 17

p pressure, atm.

Q effective charge of polyion

q velocity gradient, sec.$^{-1}$

R gas constant

R.P.M. revolutions per minute

r	radius of sphere in Stoke's law
r	inner radius of rotor in Couette apparatus
r_{ij}	distance between charges on monomer units i and j
s	number of monomers per Kuhn statistical element
T	absolute temperature, $^{\circ}K$
t	time, sec.
u_{ij}	interaction energy between charges
V	enlargement scale in Figure 17, decimeters
V_m	volume of macromolecule
V_Y	velocity in the Y-direction cm./sec.
W_o	average particle molbility of a solution at rest
$W_{\perp}$	average particle mobility perpendicular to the major axis of the particle
$W_{||}$	average particle mobility parallel to the major axis of the particle
X	direction of the velocity gradient in Couette apparatus
x	distance, cm.
Y	direction of flow in Couette apparatus
Z	direction perpendicular to the XY-plane in Couette apparatus
Z	degree of polymerization
α	degree of neutralization
α'	degree of ionization
β	angular position of a particle relative to the directional measurement of conductivity in Couette apparatus
γ	angular position of the major axis of a particle in Couette apparatus
ϵ	electronic charge, e.s.u.

η apparent viscosity, centistokes

η_o solvent viscosity, poise

η_{sp} specific viscosity

$[\eta]$ intrinsic viscosity

θ angular position of a particle relative to the directional measurement of conductivity in Couette apparatus

κ reciprocal Debye radius

μ chemical potential

μ_{el} electrostatic chemical potential

ν number of ionized groups per polyion

π osmotic pressure

ρ hydrodynamic resistance

ρ density, gm./cm.^{3}

σ q/D_r

Φ directional distribution function for the particle axes

ϕ osmotic pressure coefficient, equation (9)

ϕ angular position of the major axis of a particle in Couette apparatus, Figure 5

Subscripts

s   refers to solvent

1   refers to upper level of diffusion cell

2   refers to lower level of diffusion cell

o   refers to center of diffusion interface in diffusion cell

Superscripts

'   refers to measurements on photographic plate
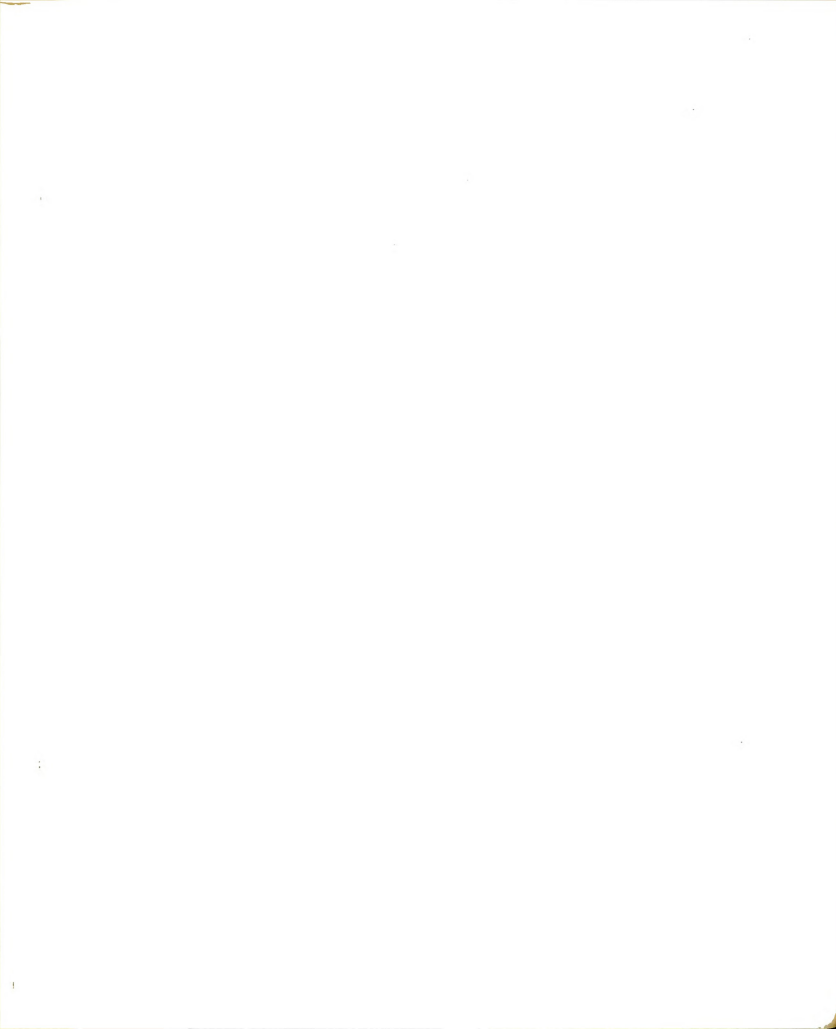
η apparent viscosity, centistokes

η_o solvent viscosity, poise

η_{sp} specific viscosity

$[\eta]$ intrinsic viscosity

θ angular position of a particle relative to the directional measurement of conductivity in Couette apparatus

κ reciprocal Debye radius

μ chemical potential

μ_{el} electrostatic chemical potential

ν number of ionized groups per polyion

π osmotic pressure

ρ hydrodynamic resistance

ρ density, $gm./cm.^3$

σ q/D_r

Φ directional distribution function for the particle axes

ϕ osmotic pressure coefficient, equation (9)

ϕ angular position of the major axis of a particle in Couette apparatus, Figure 5

Subscripts

s   refers to solvent

1   refers to upper level of diffusion cell

2   refers to lower level of diffusion cell

o   refers to center of diffusion interface in diffusion cell

Superscripts

'   refers to measurements on photographic plate